TAMPERE UNIVERSITY OF TECHNOLOGY

LAURA KANTANEN

A SCREEN FOR BIOFILM MUTANT *MYCOBACTERIUM MARINUM*

Master of Science Thesis

Examiners: Docent Mataleena Parikka and Assistant Professor Ville Santala
Examiners and topic approved on 31st of May 2017

ABSTRACT

TAMPERE UNIVERSITY OF TECHNOLOGY
Master of Science Degree Programme in Biotechnology
KANTANEN, LAURA : A SCREEN FOR BIOFILM MUTANT *MYCOBACTERIUM MARINUM*
Master of Science Thesis, 61 pages
November 2017
Major: Environmental bioengineering
Examiners: Docent Mataleena Parikka and Assistant Professor Ville Santala
Keywords: *Mycobacterium marinum*, biofilm, transduction, MycoMar T7, screening

Mycobacterium tuberculosis infects millions of people every year and in 2015 1.8 million people died from the disease. The main problem is that *M. tuberculosis* has a natural resistance to many antibiotics. Studying of *M. tuberculosis* is also problematic due to its high pathogenicity. *Mycobacterium marinum* is a close relative of *M. tuberculosis* and the *M. marinum* infection in zebrafish resembles closely the human *M. tuberculosis* infection. Therefore *M. marinum* infections on zebrafish have been used as a model for tuberculosis infections.

When grown *in vitro*, *M. tuberculosis* and *M. marinum* both form biofilms, which harbor antibiotic resistant bacteria. The biofilms are believed to be a significant contributor to the antibiotic resistance these mycobacteria. The biofilms consist of bacteria and the extracellular matrix and the main components of the extracellular matrix are proteins, lipids and extracellular DNA. In order to study the effects of the biofilm on the infection and the antibiotic resistance, biofilm mutant bacterial strains are needed.

The aim of this study was to transduct *M. marinum* with MycoMar T7 phage and screen the formed library for strains with abnormal biofilm formation. The overall experiment consisted of three screens and at each step the seemingly abnormal biofilms were selected. In the third screen the extracellular DNA and biomass contents were analyzed in reference to the bacterial count from the selected mutant strains. Crystal violet assay was used to determine the amount of biomass, DNase I was used to remove the extracellular DNA and the DNA concentrations were determined with quantitative PCR. The strains with the most interesting and promising results were then chosen for growth rate determination, where the growth rate was measured in terms of optical density and bacterial count.

As a result few highly interesting mutant strains were obtained. One of them, 2D, resembled the wild-type closely, but was unable to form a pellicle. Other very interesting strain was 8H, which produced significantly higher amounts of biofilm than the wild-type and also had remarkably low bacterial counts in cultures. Several of the other obtained mutant strains required more analyses, but could also turn out to be very interesting.

TIIVISTELMÄ

TAMPEREEN TEKNILLINEN YLIOPISTO
Biotekniikan koulutusohjelma
KANTANEN, LAURA: BIOFILMIMUTANTTIEN *MYCOBACTERIUM MARINUM* -KANTOJEN SEULONTA
Diplomityö, 61 sivua
Marraskuu 2017
Pääaine: Ympäristöbiotekniikka
Tarkastajat: Dosentti Mataleena Parikka ja apulaisprofessori Ville Santala
Avainsanat: *Mycobacterium marinum*, biofilmi, transduktio, MycoMar T7, seulonta

Mycobacterium tuberculosis infektoi miljoonia ihmisiä vuosittain ja vuonna 2015 1,8 miljoonaa ihmistä kuoli infektioonsa. Suurin ongelma *M. tuberculosis* -infektioissa on bakteerin luonnollinen resistenttiys useille antibiooteille. Tuberkuloosin tutkiminen on myöskin vaikeaa bakteerin korkean patogeenisyyden vuoksi. *Mycobacterium marinum* on fylogeneettisesti lähellä *M. tuberculosis* -bakteeria ja *M. marinum* -infektio seeprakaloissa muistuttaa läheisesti ihmisten *M. tuberculosis* -infektiota. Seeprakalojen *M. marinum* -infektioita onkin käytetty mallina tuberkuloosin tautimekanismien selvittämisessä.

In vitro -kasvatuksissa *M. marinum* muodostaa biofilmiä, jonka sisällä kasvavat bakteerit ovat resistenttejä monille antibiooteille. Biofilmin uskotaan osaltaan toimivan suojana antibiootteja vastaan. Biofilmi koostuu bakteereista ja solunulkoisesta matriisista, jonka tärkeitä komponentteja ovat proteiinit, lipidit ja solunulkoinen DNA. Jotta biofilmin vaikutuksia infektioihin ja antibioottiresistenttiyteen voidaan tutkia, tarvitaan poikkeavia biofilmejä muodostavia *M. marinum* -mutantteja.

Tämän tutkimuksen tavoitteena oli transduktoida *M. marinum* -bakteereja MycoMar T7 -faagilla ja siten luoda kirjasto, josta voidaan seuloa poikkeavaa biofilmiä tuottavia kantoja. Tutkimus koostui kaiken kaikkiaan kolmesta eri seulonnasta ja jokaisessa seulonnassa poikkeavalta näyttävää biofilmiä tuottavat kannat valittiin jatkoon. Kolmannessa seulonnassa valikoitujen kantojen solunulkoisen DNA:n ja biomassan pitoisuuksia analysoitiin ja verrattiin sitten saman kasvatuksen bakteerimäärään. Biomassan määrä määritettiin kristalliviolettilla, solunulkoinen DNA poistettiin DNaasi I:llä ja DNA-pitoisuudet kvantitoitiin kvantitatiivisella PCR:llä. Kiinnostavimmista ja lupaavimmista kannoista määritettiin niiden kasvunopeudet maljauksen ja absorbanssin avulla.

Lopputuloksena saatiin muutama erittäin kiinnostava *M. marinum* -kanta. Yksi valikoituneista mutanttikannoista, 2D, muistutti muuten villityyppiä, mutta ei tuottanut lainkaan pellikkeliä. Toinen kiinnostava kanta oli 8H, joka tuotti villityyppiä huomattavasti suurempia määriä biofilmiä, mutta jonka bakteerimäärät kasvatuksissa olivat hyvin alhaisia. Useat muista valikoituneista mutanteista saattavat myös osoittautua kiinnostaviksi mahdollisten jatkotutkimusten jälkeen.

PREFACE

The laboratory experiments described in this thesis were conducted between March 2016 and August 2017. The writing process began in spring 2017 and was finally finished in November 2017.

I want to thank the whole Infection Biology group from University of Tampere, and especially Milka Hammarén for getting me started in the lab and also for consultation even outside office hours. I had a lot of fun working in the group and I also learned a lot. I will certainly miss the humor that can only be found in the infection lab during organ block collection or infections. I would also like to thank Mataleena Parikka and Ville Santala for help with the writing process.

I would like to thank my friends and family for their support and encouragement. Especially Verner, who stood by me through the entire process.

Jyväskylä, November 9th 2017

Laura Kantanen

CONTENTS

SYMBOLS AND ABBREVIATIONS

CoA	Coenzyme A
eDNA	Extracellular DNA
GDP	Guanosine diphosphate
MHC-II	Major histocompatibility complex class II
MSO	L-methionine-*SR*-sulfoximime
NTM	Non-tuberculous mycobacteria
PE	Proline-glutamic acid
PPE	Proline-proline-glutamic acid
qPCR	Quantitative polymer chain reaction
TLR	Toll-like receptor

1. INTRODUCTION

Tuberculosis is one of the oldest known human diseases. It is caused by *Mycobacterium tuberculosis* and in 2015 10.4 million people were infected by *M. tuberculosis* and 1.8 million died from the disease [1]. The treatment of tuberculosis requires prolonged antibiotic therapy with combination of several different antibiotics. The long regime is often ended prematurely, which gives rise to multidrug resistant tuberculosis and extremely drug-resistant tuberculosis [2]. New and more efficient drugs are desperately required for treatment of the infection.

M. tuberculosis has a natural resistance to many antibiotics and one possible contributor to this resistance is the biofilm the bacteria form around them. *In vitro* the biofilm forming bacteria seem to be more resistant to antibiotics [3]. To study the effects and components of the biofilm, mutant strains with abnormal biofilms are required.

Since *M. tuberculosis* is highly pathogenic, *Mycobacterium marinum*, a close relative of *M. tuberculosis* [4], has been used to study the infection mechanisms of tuberculosis in a safer way. Zebrafish infected with *M. marinum* can be used as an *in vivo* infection model for *M. tuberculosis*. The biofilms of *M. marinum* have been studied surprisingly little, even though it is one of the closest relatives of *M. tuberculosis*.

The aim of this study is to prepare a library of *M. marinum* strains with random mutations caused by integration of MycoMar T7 phage and then screen the mutants based on the appearance of their biofilm. The ones with seemingly abnormal biofilms will be chosen. At the last stages of the experiment the amount of biofilm per bacteria will be compared between the mutants and the wild-type *M. marinum*. The strains with biofilms clearly different than the wild-type can then be used to study the effects of the biofilm on infections and resistance to biocides.

The following chapter is about the theoretical background, which first lays the basis for why this study is important and then moves on to the topics more closely related to the actual work. The third chapter describes the materials and methods used in this study. In the fourth chapter the results are presented and discussed simultaneously. This way the discussion is easier to follow, since the figures related to the results are closer and therefore easier to find. The last chapter is titled Conclusion and that chapter summarizes the whole thesis and presents the possible future experiments.

2. THEORETICAL BACKGROUND

This chapter will discuss the theory on which this thesis is based on. The chapter starts off with *M. tuberculosis* and its animal models, leading to *M. marinum* and then to comparison of the two bacteria in terms of genetics as well as infection. The chapter ends with biofilms. They are first discussed in a more general way, before the focus turns to mycobacterial biofilms and their structure and components. This way the chapter progresses from the justification of the study towards the theory of the actual topic of this thesis, which is mycobacterial biofilms.

2.1 Mycobacteria

Mycobacteria is a genus with varying natural hosts. The best known member of this group of bacteria is *Mycobacterium tuberculosis*, which causes the tuberculosis disease. The disease is usually caused by *M. tuberculosis* complex, which contains other mycobacteria as well. The mycobacteria associated with the *M. tuberculosis* complex besides the obvious *M. tuberculosis* include *Mycobacterium canettii*, *Mycobacterium africanum* and *Mycobacterium bovis* among many others [4]. The mycobacteria that are not part of the *M. tuberculosis* complex are referred to as non-tuberculous mycobacteria (NTM). However, even the NTM group includes some significant human pathogens. *Mycobacterium leprae* causes leprosy and *Mycobacterium ulcerans* causes Buruli ulcers [5]. *M. ulcerans* infection occurs mainly on skin, like *M. marinum* infections, but *M. ulcerans* can also infect bone.

In the environment non-tuberculous mycobacteria, including *M. marinum*, are often found as heterospecies biofilms [6]. The growth rate of NTM varies greatly between species. *Mycobacterium marinum* is a relatively slow-growing, even though it grows faster than *M. tuberculosis*. *Mycobacterium smegmatis* and *Mycobacterium fortuitum* are examples of fast-growing NTM [7]. There is a lot of variation between different mycobacterial species and even strains. Therefore for example biocides should be tested for each strain separately [7]. This variability between strains could partly explain the persistence of *M. tuberculosis* and other mycobacterial infections.

2.2 *Mycobacterium tuberculosis*

Tuberculosis is one of the oldest known human diseases [8]. It can affect bone, the central nervous system and many other organs, but it mainly manifests in the lungs. The infection

begins when *M. tuberculosis* reaches the lung alveolar surfaces. The bone attacking form causes deformities in the skeleton and these deformities have been discovered in 4 000 year old skeletons. It was common in ancient Egypt, but it has also been found in Neolithic sites in Italy, Denmark and Middle Eastern countries, suggesting that tuberculosis was infecting people around the world already 4 000 years ago [8].

The causative agent of the tuberculosis disease was identified by Koch in 1882 and it was named a year later as *Mycobacterium tuberculosis* [9]. In 1920's Calmette and Guerin produced an attenuated vaccine from *M. bovis* strain, which would immunize the population against tuberculosis. In 1940's the antibiotic streptomycin was discovered by Schaltz and Walksman, and this antibiotic was used to treat tuberculosis patients [8]. Later on other antibiotics were also used in the treatment of tuberculosis. The current antibiotic combination prescribed for tuberculosis typically consists of isoniazid, rifampicin, pyrazinamide and ethambutol [10]. Even though huge advances have been made, the number of tuberculosis cases is still high, especially in the developing countries [8].

2.2.1 Infection

The progression of tuberculosis infection can be divided into four stages. Around 3 to 8 weeks after *M. tuberculosis* is deposited on the alveoli the bacteria spread to lymph nodes. The lymph node infected by the bacteria forms the so called Ghon complex [8]. The Ghon complex usually resolves eventually, but it leaves signs of calcification and fibrosis, which can be seen with x-Ray [11]. During the second stage of the infection the bacteria is transported to other organs and to other parts of the lung. This stage often lasts around 3 months [8]. The third stage usually lasts 3 to 7 months and can involve severe chest pain caused by inflammation of the pleural surfaces. However, there can also be a 2 year gap between the second and the third stage. The last stage and the resolution of the Ghon complex can occur after the infection started [8]. In most cases the tuberculosis infection does not progress after the initial steps and no symptoms appear. This is called latent infection. The latent infection can reactivate after years, decades or never.

As *M. tuberculosis* enters the alveolar passages the bacteria are first phagocytosed by alveolar macrophages and dendritic cells [12]. The *M. tuberculosis* or its components are recognized by several different host receptors including Toll-like receptors (TLR) and C-type-lectins [12]. The phagocytosed bacteria are placed in an endocytic vacuole called phagosome. As the *M. tuberculosis* enters the host, its metabolism changes. When grown *in vitro M. tuberculosis* prefers carbohydrates as energy source but *in vivo* it uses fatty acids as the preferred energy source [8].

In normal phagosome maturation cycle the phagosome would fuse with lysosome and the bacteria would be destroyed by acid pH, reactive oxygen intermediates, lysosomal enzymes and toxic peptides [8]. However, *M. tuberculosis* is able to survive within the phagosome and to prevent the phagosome maturation and the fusion of the phagosome

with the lysosome [13]. The proton ATPases are excluded from mycobacterial phagosomes and this is believed to prevent their acidification [8]. The live phagocytosed *M. tuberculosis* also prevents increases in Ca^{2+} levels, which are associated with the fusion of phagosome and lysosome [14]. Several immune responses are also stimulated by Ca^{2+}, so the limited Ca^{2+} levels help *M. tuberculosis* to protect itself from the host's immune responses [8]. The phagosomes containing *M. tuberculosis* express Rab5, which is a protein associated with early endosomes. These phagosomes therefore do not recruit Rab7, which is a protein associated with more mature endosomes [15]. However, it is not yet known whether the lower Ca^{2+} levels and/or the Rab7 exclusion are required to stop phagosome maturation or if they result from it [8]. By residing within the phagosome, the bacteria are hidden from the $CD4^{+}$T cells and as a possible result the expression of the major histocompatibility complex class II (MHC-II) proteins is decreased, as well as the presentation of MHC-II bacterial antigens [16]. A secreted or surface exposed *M. tuberculosis* lipoprotein, sometimes referred to by its size as 19-kDa, is believed to interact with TLR2 when the bacteria enter the macrophages [8].

In the next steps of the *M. tuberculosis* infection the bacteria residing in the macrophages attract inactivated monocytes, lymphocytes and neutrophils. None of these are able to kill the bacteria and clear the infection. Instead these cells are used to form a granuloma and the bacteria are contained within it. Within the granulomas the bacteria spreads from infected macrophages to uninfected macrophages [13]. The beginning of granuloma formation correlates with rising bacterial count [17]. Mature established granulomas are porous allowing entry of the bacteria to the already established granuloma [18]. Cellular immunity helps to destroy the infected macrophages creating the caseous, necrotic center of the granuloma [8]. Even though granulomas limit the growth of *M. tuberculosis*, it is obvious that the mycobacterium has evolved to take advantage of them and use them as a protection against the host immune system [13]. The *M. tuberculosis* bacteria residing in the granuloma may enter dormancy and they can remain dormant for decades. The bacteria are most likely dying and dividing at same rate so the bacterial count remains constant. This is the basis of the latent *M. tuberculosis* infection, which is asymptomatic and nontransmissible [8].

If the immunity of the host remains uncompromised, the infection may stop here and the granulomas eventually heal so that only small fibrous and calcified lesions remain. This is often referred to as cleared latent infection. However, if the host's immune system becomes compromised, the center of the granuloma may become liquefied serving as a rich medium for the reviving bacteria. The revived *M. tuberculosis* can escape the granuloma and spread within the lungs or to other organs resulting in an active infection [8]. Since the overall health affects the immune system, tuberculosis flourishes in malnourished and overcrowded populations.

Extensive growth of *M. tuberculosis* in the lungs causes severe lung damage and even-

tually leads to death by suffocation [8]. The amount of lung parenchymal cells, which are involved in oxygen intake, is significantly reduced close to none, the bronchiolar passages are blocked by granulomas and the rupture of liquefied granulomas releases blood to the lung tissue, all of these leading to suffocation [8]. The tissue damage associated with *M. tuberculosis* infection is mainly caused by inflammatory host responses. Proteases are believed to be responsible for liquefication of granulomas and to cause the tissue damage. The phagocytosis of *M. tuberculosis* can also lead to apoptosis of the macrophages, which also may result as tissue damage. The tumor necrosis factor α (TNF-α) cytokine is a part of the inflammatory response and necessary for infection control [8]. In mice it is required for granuloma formation, but in large amounts it will cause severe lung inflammation and early death. A clinical *M. tuberculosis* strain, CDC1551, was thought to have exceptionally high virulence. Since virulence is defined by mortality and bacterial loads, the strain did not have higher virulence than others. However, it induces significantly higher levels of cytokines, including TNF-α, leading to a seemingly more virulent phenotype [8]. It seems that in some cases the apoptosis of the macrophages is dependent on TNF-α and that the more virulent *M. tuberculosis* strains induces lower levels of TNF-α, leading to less apoptosis [8]. There are also other factors besides TNF-α that affect the progression of the tuberculosis.

2.2.2 Virulence

There are several proteins believed to be linked to *M. tuberculosis* virulence and growth within human host. One of them is HspX, which is a 16-kDa protein found in the *M. tuberculosis* culture filtrate, but it is also recognized by sera of tuberculosis patients, suggesting it is produced during infection in humans. The production of the protein is induced under anoxic conditions and in human THP-1 macrophages. The protein might have a chaperone-like function and it could be involved in latency control [8]. The previously mentioned 19-kDa protein is also recognized by sera of tuberculosis patients as well as the T cells and it is believed to initiate a host signaling pathway by interaction with TLR2. Several studies have been conducted regarding the 19-kDa protein. It seems that the protein might induce different signaling pathways depending on the cell, which it is interacting with [8].

ESAT-6 (6 kDa early secreted antigenic target) and CFP-10 (10 kDA culture filtrate protein) are also *M. tuberculosis* culture filtrate proteins and recognized by sera of tuberculosis patients [8, 13, 19]. These proteins are expressed from the ESX-1 locus, which is removed from the attenuated *M. bovis* strain (*M. bovis BCG*) used for *M. tuberculosis* vaccination [19]. The two proteins are co-secreted with a third protein called EspA, which lies outside of the ESX-1 locus [13]. A fourth protein, EspB, is secreted when CFP-10 is not present [20]. The ESAT-6 has been suggested to be a signal that induces secretion of matrix metalloproteinase Mmp9 in epithelial cells. Mmp9 facilitates the recruitment

of macrophages and therefore promotes the expansion of the granuloma [21]. A functional ESX secretion system is required for phagosome maturation arrest [22] and the phagosomal escape is also dependent on the ESX-1 secretion system [13]. The ESX-5 secretion system is required for secretion of proteins of proline-glutamic acid (PE) and proline-proline-glutamic acid (PPE) families, but the functions of these families remain partly unknown [23]. Some of the PE and PPE proteins are located on the cell surface and some are known to interact with the host immune system.

Glutamine synthase is also found in *M. tuberculosis* culture filtrate, but this is believed to be a result of cell leakage and lysis. Inhibition of this enzyme by L-methionine-*SR*-sulfoximime (MSO) also inhibits *M. tuberculosis* growth both *in vitro* and *in vivo*, but the inhibitor has no effect on nonpathogenic mycobacteria. In *M. tuberculosis* the glutamine synthase is known to be involved in the synthesis of poly-L-glutamate-glutamine, which is a cell wall component of pathogenic mycobacteria [8].

Not all virulence factors of *M. tuberculosis* are secreted. The cell surface of *M. tuberculosis* contains several proteins and other components that affect the virulence of the bacterium [8]. One of these proteins is Erp. It is not found in non-pathogenic mycobacteria and a mutation in this gene leads to an attenuated infection in cultured macrophages and animal models and also to higher susceptibility to detergents [8, 13]. The exact function of the protein is still unknown, but it is known to interact with two proteins located on the cell membrane of *M. tuberculosis*. The other one of these proteins is not present in NTM [24]. However, Erp can be found in other pathogenic mycobacteria as well. HbhA is also a protein found on the cell surface of *M. tuberculosis*. It is a heparin binding hemagglutin protein found in pathogenic mycobacteria. Mutants lacking HbhA interact normally with macrophages, but they do not interact with pneumocytes [25]. It seems that HbhA plays more important role in extrapulmonary tuberculosis.

Some *M. tuberculosis* cell wall lipids, like phthiocerol dimycocerosate, trehalose dimycolate and phenolic glycolipids, have been identified as important determinants of virulence [13]. In cultured macrophages purified and cyclopropane modified trehalose dimycolate induces pulmonary granulomas and phenolic glycolipids inhibit the release of proinflammatory cytokines [13]. Lipoarabinomannan is also an important virulence factor. It downregulates the host's responses to *M. tuberculosis* infection in several ways [8]. Several of the cell wall lipids interact directly with the host immune system enabling the *M. tuberculosis* to survive and replicate. Several enzymes have also been identified as essential for *M. tuberculosis* virulence. Many of these are involved in the synthesis of phthiocerol dimycocerosate or located near the gene cluster involved in the synthesis [8]. It seems that phthiocerol dimycocerosate is an important factor in *M. tuberculosis* virulence and mutations that disrupt or reduce its synthesis would result in attenuated infection phenotypes. Enzymes involved in production of other cell wall lipids have also been linked to *M. tuberculosis* virulence [8]. At least some of these lipids are only present in the cell

walls of pathogenic mycobacteria. The composition of mycobacterial cell wall will be discussed later in greater detail.

2.2.3 Zebrafish as an infection model for tuberculosis

There are a few mammalian animal models developed for *M. tuberculosis* infection. Mice form only poorly organized and non-caseating macrophage aggregates [26]. The best resemblance with granuloma pathology of humans has been achieved in macaques and macaques also have both the active and latent state of the disease [13]. However, the use of macaques is quite unethical and also costly. Mice have also been used as a model of *M. marinum* infections, but the bacterial count decreases over time and the granulomas remain non-caseating [13]. An interesting result found in mouse studies is that *M. marinum* immunization offers protection against *M. tuberculosis* [27]. This is an interesting result, since it could be a proof of close resemblance between the two bacteria. The resemblances between *M. tuberculosis* and *M. marinum* will be discussed further later.

Zebrafish on the other hand develop a symptomatic wasting *M. marinum* infection with caseating granulomas resembling the granulomas of active human tuberculosis [13]. The granulomas in zebrafish are usually multi-centric and surrounded by a fibrous capsule [28]. Another advantage with zebrafish as an infection model is the genetic variability, which mimics the genetic variability in the human population. The genetic background affects the individual's ability to control and clear the infection and in heterogeneous zebrafish population the effects of genetic variance can be studied [29]. Zebrafish are also small, quite inexpensive and easy and fast to breed.

Zebrafish have both innate and adaptive immunity with conserved orthologues of key human immune molecules [30]. The adaptive immunity develops later than the innate immunity, like in mammals. T cells appear in the thymus 3 days after fertilization, but the functional T cells exit the thymus only three weeks after fertilization [13]. This gives a chance to study the effects of innate immunity alone by infecting the zebrafish only a few days after the fertilization. Zebrafish larvae express a wide variety of toll-like receptors, which generally play an important role in innate immunity, and some of these receptors are induced during *M. marinum* infection [13]. Two types of genes, structurally related to Ig-type receptors and C-type lectin receptors found in mammalian natural killer cells, are expressed in zebrafish and these receptors are believed to contribute to the innate immunity [31]. *M. marinum* is phagocytosed within 1 h after intravenous injection into 30 h old zebrafish embryos. However, the embryonic macrophages are unable to eradicate the bacteria. The pro-inflammatory cytokines TNF and IL-1β are induced within first 24 h [32]. The infected macrophages aggregate within 4 days and form structures resembling granulomas [13]. The granuloma formation does not therefore require adaptive immunity responses. However, the adaptive immunity response is required for proper control of the infection, since the rag1 mutants are hypersusceptible to *M. marinum* infections [33]. The

innate mechanisms seem to mainly modulate the inflammatory and bactericidal response to infection [34].

M. marinum infection in zebrafish can either manifest as an acute infection or as a chronic progressive disease. The acute infection leads rapidly to lethal inflammation, but the chronic diseases progresses slower and usually leads eventually to abdominal swelling, uncoordinated swimming, weight loss, hemorrhages and skin ulcerations [35, 36]. Before visible symptoms in zebrafish granulomas develop in organs, such as liver, spleen, kidney, pancreas and intestines [29]. The organ block can be collected and the *M. marinum* load determined with quantitative PCR (qPCR). Zebrafish can also be used to mimic a latent *M. tuberculosis* infection. This model can be achieved with low bacterial loads in infection [28]. After several weeks the bacterial counts become stable and the number of granulomas remains constant. This latency relies on rag1-mediated adaptive immunity. The bacteria residing in granulomas becomes dormant. The infection can be reactivated with immunosuppression induced by gamma irradiation [28].

Embryonic zebrafish are transparent, which enables real time monitoring of *M. marinum* infection *in vivo*, especially when fluorescent bacteria are used. With the use of low concentrations of 1-phenyl-2-thiourea the zebrafish larvae will also remain transparent [37]. Modified antisense oligonucleotides, morpholinos, designed to inhibit mRNA translation or splicing, can be used for reversed genetics in in zebrafish embryos and larvae [13]. This enables studies with altered phenotypes. Retroviral insertions can also be used to identify germline mutants in specific genes [13]. Similar effects to the knockdown of CCL2-CCR2 signaling, which is associated with macrophages recruitment, can be achieved in zebrafish with mutations of cxcr3.2, which is a homologue of human CXCR3 receptor [38].

2.3 *Mycobacterium marinum*

Mycobacterium marinum is an NTM found in both fresh and saltwater. It is a slow growing mycobacterium, but its generation time is significantly shorter than the generation time of *M. tuberculosis* [13]. The optimal growth temperature for *M. marinum* is below 30 °C. *M. marinum* was first discovered in 1926 in an aquarium from dead saltwater fish [39]. It infects mainly fish, but can also cause a skin infection in humans. The first identified human *M. marinum* infection was reported in Sweden in 1951 by Norden and Linell [39]. In fish the infection resembles the human tuberculosis infection. For the infection to occur in humans, *M. marinum* requires an access to the bloodstream via injured skin. In humans the symptoms are milder and occur usually only on the surface of the skin in the outer limbs. This is most likely a result of the lower optimal growth temperature, since hands and feet tend to have lower temperature than the core body. The *M. marinum* infection in humans is often referred to as fish tank or swimming pool granuloma. In immunocompromised individuals the disease can, however, resemble more

closely *M. tuberculosis* infection. The *M. marinum* infection results in fish and humans as similar granulomas as associated with *M. tuberculosis* infections. Since *M. marinum* and *M. tuberculosis* are closely related *M. marinum* along with other NTM has been used to study mycobacterial infection mechanisms, which could be shared with *M. tuberculosis*. As stated in the previous section, the zebrafish has been used as a model organism in *M. marinum* studies.

2.3.1 Infection

It is not yet completely understood how *M. marinum* enters its natural host, fish, and begins the infection. The two main ideas at the moment seem to be via the gastrointestinal system or by the gills. However, by injecting *M. marinum* to the caudal vein of zebrafish embryos, the early events of *M. marinum* infection in zebrafish can be studied [40]. The injected bacteria were immediately phagocytosed by blood macrophages. The bacteria are able to transfer between two macrophages and the infected macrophages can be phagocytosed by uninfected ones, which will then become infected [40]. Within 1 day the infected macrophages had been spread to different tissues. In zebrafish embryos the bacteria was phagocytosed only by macrophages, but with adaptive immune system, other cells are likely also involved in the establishment of the infection.

3 days after the injection, the infected macrophages located in the tissues of the embryo start to form aggregates, which would eventually turn into granulomas. The aggregated cells are squeezed together tightly and new cells are added to the aggregates [40]. The aggregates in zebrafish embryos consist solely of macrophages and the membranes of these cells were tightly packed next to one another or the cell boundaries were indistinct. The granulomas contain also uninfected cells. The bacteria resides both intracellularly in the aggregates and extracellularly in the necrotic center [40]. The number of bacteria residing in a necrotic centers varies greatly between granulomas. High initial bacterial loads killed the embryos within 6 to 9 days. Heat-killed *M. marinum* is phagocytosed by macrophages in similar manner, but the bacteria is degraded within 2 days [40]. Different *M. marinum* genes are activated upon phagocytosis and in aggregated macrophages in adult zebrafish. The same genes were also activated in the zebrafish embryos in corresponding situations [40]. This shows that the macrophage aggregates in the embryos resemble the granulomas found in adult zebrafish.

In very low bacterial concentrations of *M. marinum* containing phthiocerol dimycocerosates can use the CCL2-CCR2 chemokine signaling axis to recruit permissive macrophages in a phenolic glycolipid dependent way [41]. CCR2 is required to mobilize the monocytes from the bone marrow and to move them to the inflammation site [42] and at least in murine models CCR2 deficiency impairs the host defense [29]. The CCL2 is generally considered as an inflammatory chemokine, but it can also change the polarization of macrophages closer to an anti-inflammatory phenotype [43]. The high expression

of CCL2 also seems to correlate with susceptibility to tuberculosis [44].

2.3.2 Virulence

The ESX system is important for *M. marinum* virulence. The ESAT-6 and CFP-10 proteins are co-secreted with EspB [22]. The function of the ESAT-6 is believed to be similar in both *M. marinum* and *M. tuberculosis*, so it is believed to induce a signal that results in expansion of granulomas by recruitment of macrophages [21]. The *M. marinum esx-1* mutants are phagocytosed normally and replicate within the macrophage normally, but they fail to form granulomas [17]. Mutations in the *M. marinum* ESX-1 secretion system also prevent phagosomal escape and the resulting cytosolic actin polymerization and cell to cell spread [13]. Phagosome maturation arrest also requires a functional ESX secretion system [22]. The ESX-1 secretion system seems to promote macrophage aggregates and therefore the granuloma formation.

The ESX-5 secretion system is required for secretion of proteins of proline-glutamic acid (PE) and proline-proline-glutamic acid (PPE) families, but the functions of these families remain partly unknown [23]. Some of the PE and PPE proteins are located on the cell surface of *M. marinum* and they are known to interact with the host immune system. The ESX-5 mutants of *M. marinum* cause different infection phenotypes in embryos and in adult zebrafish. In embryos the infection phenotype is a bit attenuated, but in adults it is hypervirulent [23]. The difference could be caused by the adaptive immunity, which the embryos lack, however, the ESX-5 mutants grew better even in *rag1* mutant adult zebrafish, suggesting that the difference in infection phenotypes lies elsewhere. It seems that *M. marinum* requires the ESX-5 secretion system for establishment of persistent infection [29]. The same study [23] also showed that it is useful and occasionally even necessary to use both embryos and adults before proper conclusions can be made.

Mutation in the *erp* gene causes an attenuated infection in cultured macrophages and animal models and also higher susceptibility to rifampicin [13]. These mutants seemed to be phagocytosed normally, but they are unable to survive within the macrophages [45]. A depletion of macrophages normalizes the infection phenotype, suggesting that the secreted surface protein *erp* encodes only interacts with macrophages [32]. On the other hand, a mycobacterial infection lacking macrophages can hardly be called normal, since macrophages seem to be a vital part of the infection mechanism. Another gene affecting the infection phenotype is *iipA*. A mutation in the *iipA* gene affects the cell wall structure of *M. marinum* leading to higher antibiotic susceptibility [13]. The gene contains highly conserved domains that are believed to mediate peptidoglycanase activity. These mutants form deficient biofilms and their invasion and intracellular survival are defective, leading to an attenuated infection [13].

2.4 Comparison between *M. marinum* and *M. tuberculosis*

M. tuberculosis and *M. marinum* are closely related mycobacteria that infect macrophages and cause a chronic and systemic disease [13]. However, their natural hosts are very different. The natural host of *M. tuberculosis* is human, but for *M. marinum* it is ectotherms like fish and frogs [13]. The optimal growth temperatures are also different, correlating with the natural hosts. The optimal growth temperature for *M. marinum* is below 30 °C and for *M. tuberculosis* it is around 37 °C.

The generation time during logarithmic growth of *M. marinum* is 4 h, which is significantly shorter than the generation time of over 20 h of *M. tuberculosis* [13]. *M. marinum* forms visible colonies on agar in a week, but *M. tuberculosis* requires three weeks [36]. Despite the differences in natural hosts and generation times, the genetic programs are well conserved between the two bacteria and therefore they have many shared determinants of virulence [13]. The faster growth combined with lesser threat to humans make *M. marinum* an interesting model organism for *M. tuberculosis* studies.

2.4.1 Genetics

The *M. tuberculosis* genome is only two thirds of the *M. marinum* genome, which is 6.6 Mbp and it is possible that most of the difference in the genome sizes is due to a loss of genetic material in *M. tuberculosis* [13]. As *M. tuberculosis* specialized to survive mainly intracellularly, it may have lost genes that are important for extracellular survival. An example is the light induced beta-carotene production in *M. marinum*, which turns the bacterial cultures yellow. It protects the bacteria from photo-oxidation damage [46]. The photochromogenicity of *M. marinum* has also been linked to intracellular survival, since disruption of a region between two genes, which have homologues in *M. tuberculosis* increases the susceptibility to singlet oxygen and decreases the survival in macrophages [47].

Besides losses in the *M. tuberculosis* genome, *M. marinum* has also acquired new loci via gene duplication and lateral gene transfer after the divergence from *M. tuberculosis* [48]. 14 % of the *M. tuberculosis* genome is not shared with *M. marinum* [48], but this part is hypothesized to be mostly related to host transmission and organ specificity instead of central pathogenesis mechanisms [13]. The identity between the *M. marinum* genome with the orthologous regions of the M. tuberculosis genome is 85 % and the coding sequence amino acid identity is also around 85 % between orthologues [48]. *M. marinum* and *M. tuberculosis* have orthologous virulence determinants and the *M. tuberculosis* orthologues are able to compliment the *M. marinum* virulence determinants, suggesting a conserved function [13].

An example of the shared virulence determinants are ESAT-6 and CFP-10, which are secreted from the ESX locus. These two proteins are secreted virulence determinants

found in *M. marinum* and *M. tuberculosis*. In both bacteria they are co-secreted with a third protein, which is different between the two bacterial species. In both bacteria the ESX secretion system is required for phagosome maturation arrest and phagosomal escape. The conserved virulence determinants and similarities between the genetic programs of intracellular growth and host survival suggest that the common ancestor of *M. marinum* and *M. tuberculosis* was able to colonize in vertebrates with at least some kind of primitive adaptive immune system [13].

2.4.2 Granulomas

In *M. tuberculosis* infection, as well as in *M. marinum* infection, the bacteria are phagocytosed by host macrophages, but this does not actually help to eradicate the infection [13]. Both bacteria are able to survive and even replicate within the macrophages [49]. In fact the phagocytosis is actually part of the survival plan of the bacteria. Mycobacteria use the lipids of their outer cell wall to manipulate the macrophage [36]. The infected macrophages migrate into tissues and aggregate into complex granulomas [13]. The structures of the granulomas as well as their assembling mechanisms are similar in both bacteria. The cells are tightly packed and the boundaries between cells can be come indistinguishable [40]. The acellular necrotic core is called caseum. The mycobacteria reside within the caseum extracellularly [13] or inside the infected macrophages [40]. Even though granulomas limit the growth of mycobacteria, it is obvious that the pathogenic mycobacteria have evolved to take advantage of them and use them as a protection against the host immune system [13]. *M. tuberculosis* can persist inside granulomas for decades as a latent infection [50]. When the granuloma integrity is lost, the latent infection becomes active and the disease can be transmitted further [29].

The phagocytosis induces specific gene expression patterns in both *M. marinum* and *M. tuberculosis*. When these patterns were studied in *M. marinum*, most of the identified genes had orthologues in *M. tuberculosis*. However, the genes were constitutively expressed *in vivo* in *M. tuberculosis* undoubtedly due to the intracellular survival tactic, although the pathogenesis mechanisms may also affect [13]. As *M. marinum* is able to survive both intracellularly and in the environment, the transitions require changes in gene expression. These two alternating states partly explain the larger genome of *M. marinum*. Since the niche of *M. tuberculosis* is restricted to host, there is less need for gene regulation [13].

M. marinum and *M. tuberculosis*, like many other pathogenic mycobacteria, arrest the phagosome maturation before the phagolysosome fusion [13]. It is only live *M. marinum*, not dead, that prevents the fusion of macrophage and lysosome [36]. *M. marinum* localize themselves to non-acidified phagosomes excluding the vacuolar proton ATPase [13]. This has been hypothesized to act as a protection against phagolysosome mediated killing. It might also offer *M. marinum* a chance to alter the antigen presentation and therefore

the adaptive immune response of the host [51]. *M. marinum* is also able to escape from phagosomes to cytosol and develop an actin-based motility [52]. This escape has also been suggested to occur in *M. tuberculosis* infections but the results are considered as controversial [13]. It is possible that the phagosome escape of *M. tuberculosis* is under tighter regulation than in *M. marinum* and therefore it has not been documented as well [36]. However, *M. tuberculosis* does not have the actin based motility of *M. marinum* or other means to propel itself outside host cells. The actin based motility of *M. marinum* is believed to be used in the initial stages of infection and it has not been observed in other mycobacteria, not even in *M. ulcerans*, which is the closest relative to *M. marinum* [36].

The dermal *M. tuberculosis* granulomas and the *M. marinum* granulomas are usually indistinguishable in humans, since they both have a lymphocytic cuff surrounding epithelioid cells and the necrotic core in the center [13]. The *M. marinum* induced granulomas in fish have very few lymphocytes, but these lymphocytes are important in restriction of the bacterial growth [13]. The histopathologies of mature granulomas have more variation between different hosts than between *M. marinum* and *M. tuberculosis* infections [13]. The *M. tuberculosis* infection in humans resembles the *M. marinum* infection in zebrafish more than the *M. tuberculosis* infection in mice. It's an interesting notion, since mycobacterial infections use the host immune system to their advantage and therefore the immune system has also a great impact on the infection.

2.5 Biofilms

All bacteria, including mycobacteria, typically form biofilm [6]. These biofilms consist of bacteria and extracellular matrix (ECM) produced by the bacteria. The biofilms are either attached to a biotic or abiotic surface or suspended as flocks [7, 53]. Biofilms are practically present everywhere. Currently one of the most harmful ones, possible excluding the infectious biofilms within human body, are the biofilms present on medical equipment. Biofilms can also be used to our advantage. For example in water treatment plants biological water treatment is usually based on biofilms, because bacteria residing in biofilms are more resistant than planktonic bacteria, which would just be washed away with the treated water.

Biofilms offer bacteria several advantages and therefore biofilms have most likely evolved as a survival tactic. One of the advantages is resistance to environmental threats. These threats include antibiotics, biocides and other sterilization agents. For example biofilms of NTM are highly tolerant to chlorine [6]. The biofilms attached to the surface are not washed away as easily as planktonic bacteria. Biofilms also protect the bacteria from phagocytosis and other immune responses, which makes biofilm associated infections more persistent and less responsive to antibiotics. The bacteria residing in biofilms are dispersed as flocks and therefore they are more potent to spread infections. Even

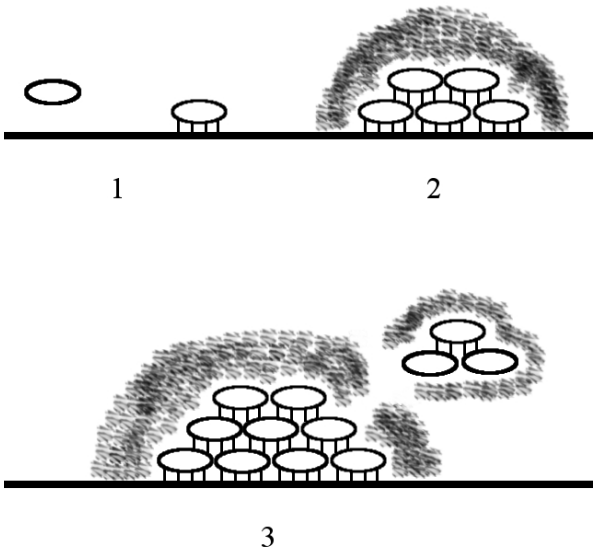

Figure 2.1: The steps of biofilm formation. The steps have been numbered and the first one is attachment of the bacterium to the surface. The second step is bacterial division and formation of the extracellular matrix and the third one is dispersal of the bacteria from the mature biofilm as flocks.

though biofilms protect the bacteria from host immunity and enable more efficient spreading of the infection, they are not a direct sign of pathogenesis. Many non-pathogenic bacteria, too, form biofilms [53].

The formation of biofilm is a genetically controlled process with several steps [6]. These steps are illustrated in figure 2.1. The biofilm formation begins typically by attachment to the surface and this attachment is usually mediated by filaments, which extend from the bacteria [54]. The attachment is followed by bacterial division and the synthesis of the ECM. Once the biofilm is mature, the bacteria can disperse from it as small flocks and form biofilms at new locations [6].

The biofilm forming bacteria usually grow in a sigmoidal fashion [7]. It is reasonable to assume that at first bacteria form the biofilm to protect themselves and only then they start to divide. After the stable biofilm has been formed, the bacteria most likely concentrate their resources on biofilm formation and therefore the bacteria are metabolically active but not actively dividing. *M. tuberculosis* biofilms are unaffected by attacks against cell wall biosynthesis, which could be a sign of reduced cell division [55].

Biofilms protect the bacteria from environmental conditions and antimicrobials. The bacteria living in the center of the biofilm do still require nutrients and oxygen. Therefore there are water channels in the biofilm, which are used to transport molecules in and out

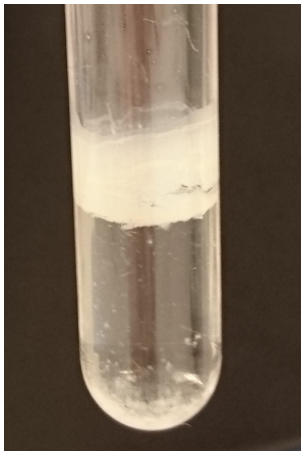

Figure 2.2: A wild-type *M. marinum* pellicle. In this culture the pellicle at the air-liquid interphase is significantly larger than the pellet found at the bottom.

of the biofilm [7, 56].

Biofilms contain several microenvironments. The growth conditions are naturally very different deep inside the biofilm compared to the outer surface of it. Bacteria adapt to these microenvironments both physiologically and metabolically and therefore the bacteria within the same biofilm are phenotypically heterogeneous, even though they have the same genotype [57]. The heterogenicity is an advantage for the bacteria, possibly offering quicker responses to sudden conditional changes. The different microenvironments also affect the cell length, which has been linked to phenotypic drug tolerance [6]. Impaired biofilms of mixed *M. tuberculosis* mutants are more susceptible to antibiotics than the wild-type biofilms [6], making the different phenotypes more relevant than different genotypes. Also in biofilm the bacteria can work together by dividing the production of the ECM molecules. This would require quorum sensing. Some research about quorum sensing and its link to biofilms has been done, but several unanswered questions still remain [58].

2.5.1 Mycobacterial biofilms

The mycobacteria have a strong tendency to form biofilms in liquid cultures [6]. The mycobacterial biofilms are usually attached to the bottom and to the sides of the culture container. The biofilms attached to the bottom are generally referred to as a pellet and the biofilm that forms in the air-liquid interphase is called pellicle. The pellicle is usually attached to sides of the container. Figure 2.2 shows a large *M. marinum* pellicle at the air-liquid interphase and a relatively small pellet at the bottom. The attachment of the pellicle to the sides of the container can also be seen clearly in the picture. Detergents, such as Tween®80, can be used to reduce the biofilm formation and to grow more dispersed cultures [6]. If the bacterial culture requires dilution before use, which would be the case,

if the bacteria would be used for infection experiment, the dispersed cultures result in more accurate dilution series.

The mycobacterial biofilms contain several different lipids. These lipids have been suggested to form a hydrophobic film between the bacteria and the hydrophilic agar surface [59]. This would reduce the interaction between bacteria and the agar and enable the sliding motility of the bacteria. The interaction between two hydrophilic surfaces is stronger and therefore the sliding would require more energy, since breaking the interaction between the two surfaces would require more energy. The lipids also facilitate in attachment since they make the outer surface of the bacteria more hydrophobic and therefore allow the attachment to the hydrophobic surfaces, like PVC [60].

The morphologies of biofilms vary between species. The fast-growing *Mycobacterium fortuitum* aggregates as heterogeneous filaments, where extracellular polymeric substances are clearly visible [7]. *M. marinum* on the other hand forms more typical microcolonies, with individual bacteria and extracellular polymeric substances less prominent and visible [7].

There are certain conditions that promote the formation of biofilm. Incubation of *Mycobacterium avium* ssp. *hominissuis* in subinhibitory concentrations of streptomycin and tetracycline induces the biofilm formation [61]. It is reasonable that low concentrations of antibiotics would increase the biofilm formation, since the biofilm can be used to protect the bacteria. Also the biofilm formation in *M. avium* seems to be dependent on Ca^{2+}, Mg^{2+} or Zn^{2+} ions, but the concentrations of the ions do not affect the biofilm formation significantly, only their presence [59]. 2 % concentration of peptone and glucose also induces the biofilm formation but humic acid was partially inhibiting [59].

In *M. avium* strains biofilm formation is more efficient in water than in 7H9 broth, which is a commonly used mycobacterial medium [59]. Also in *M. tuberculosis* cultures low nutrient and oxygen concentrations induce formation of non-replicating but viable and drug tolerant bacteria [6]. The non-replicating bacteria are most likely actively forming biofilm. The scarce nutrients may be concentrated into the biofilm and utilized by the bacteria. Also a liquid media lacking salts may cause the cells to explode but inside the biofilm the environment can be more concentrated, preventing the leakage of molecules from the cell to the medium.

Biofilms have also direct effect on the virulence of mycobacteria. Biofilm defective *M. avium* mutants are unable to colonize and translocate through bronchial epithelial cells resulting in an attenuated infection [59]. Also the ECM of *M. ulcerans* biofilm contains vast amounts of mycolactone, which is an extracellular toxin and the major virulence factor of *M. ulcerans*, rendering the sterilized biofilm toxic as well [62]. UV-sterilized biofilm of *M. avium* subsp. *hominissuis* stimulates the macrophages in a same way as the non-sterilized biofilms did [63]. It seems that a component of the *M. avium* subsp. *hominissuis* biofilm matrix induces the cell death of the macrophages instead of live bac-

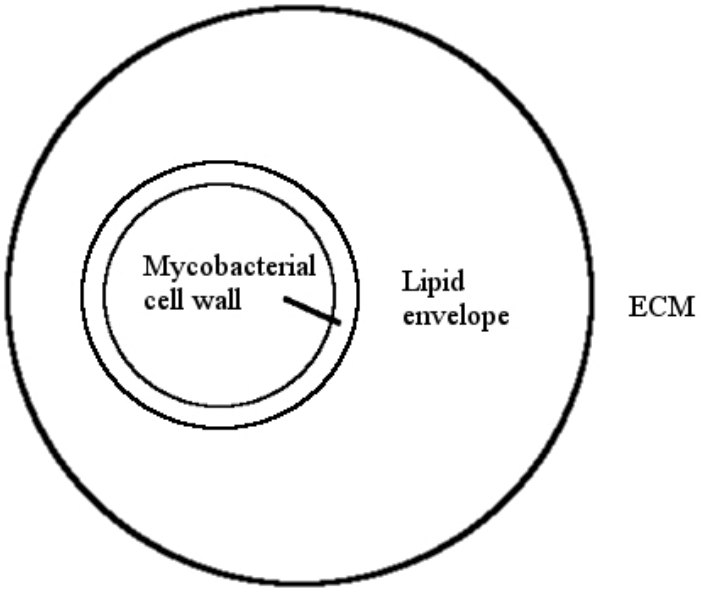

Figure 2.3: A simplified model of the structure of a typical mycobacterial biofilm. The cell is surrounded by lipid envelope, and the envelope is surrounded by the extracellular matrix (ECM). The ECM separates the bacteria from the environment.

teria.

Most of the mycobacteria form structures called cords, when they grow extracellularly [13, 64]. In cords the bacteria are aligned parallel to each other along the long axis of the cord forming string-like structures [65]. These were originally linked to virulence, since in *M. tuberculosis* only virulent strains form cording structures [13]. However, they were later found from non-pathogenic mycobacteria as well [64]. There seems to be a link between cording structures and virulence in *M. marinum* as well [13]. *M. marinum kasB* mutants, which will be discussed in more detail later, have defects in cord formation and cause an attenuated infection in zebrafish [66].

With mycobacterial biofilms it must be taken into consideration that the differences between *in vitro* and *in vivo* biofilms can be massive. As an example, it was determined that *mag5* gene, which is an *M. marinum* virulence determinant, was expressed at a low level in cultured macrophages, but strongly activated in zebrafish embryos [40]. It seems that the microenvironments within macrophages *in vivo* have a lot more variation than can be simulated *in vitro*.

A simplified structure of an *in vitro* mycobacterial biofilm is shown in figure 2.3. The mycobacterium is surrounded by lipid envelope, which is sometimes referred to as cell envelope as well. Outside the lipid envelope is the extracellular matrix of the biofilm. The lipid envelope is sometimes considered as part of the cell wall or as part of the extracellular matrix. It appears to be somewhat difficult to point out in which parts of this biofilm

structure certain molecules are found. The cell wall, lipid envelope and the extracellular matrix will be discussed further in following sections.

Many of the biofilm characteristics are shared among different mycobacteria, possibly partly due to the similar cell wall structure. The biofilms of *M. marinum* have been studied surprisingly little, even though *M. marinum* is the one of the closest relatives of *M. tuberculosis*. Also the availability of *in vivo* models for *M. marinum* studies make it an interesting research topic.

2.5.2 Mycobacterial cell wall and the lipid envelope

Mycobacteria are classified as gram-positive, even though their cell wall contains some characteristic of the cell walls of gram-negative bacteria as well [67]. The structure of the mycobacterial cell wall is quite unique and a feature that can be used to set the mycobacteria apart from other bacteria. The mycobacterial cell wall contains an outer permeability barrier, which acts like an outer membrane, but is not really one [67].

The core structure of the cell wall consists of mycolyl-arabinogalactan-peptidoglycan molecules and it was discovered already back in 1982 by Minnikin [67]. The parts of the molecule, mycolic acid, arabinogalactan and peptidoglycan, are covalently linked to one another [68]. Mycolic acids are bound to the arabinogalactan polysaccharide layer [60]. These mycolic acids are largely responsible for the antimicrobial protection [54].

The mycobacterial cell wall is surrounded by an envelope consisting of various lipids. This envelope is sometimes referred to as part of the cell wall and sometimes it is thought to be part of the biofilm. This outer layer of the cell wall, or envelope, consists of solvent extractable lipids that intercalate with mycolic acids [68]. The structure of these lipids varies between mycobacterial species. The glycolipids found in mycobacterial envelopes include glycopeptidolipids, lipoarabinomannan, lipomannan, phthiocerol dimycocerosates, lipooligosaccharides, phenolic glycolipids and trehalose dimycolate [68].

In mycobacterial biofilms the correct cell wall structure is the basis of biofilm formation and therefore cell wall biosynthesis is very important for proper biofilm formation [5]. Defects in cell wall structures cause defects in biofilms. Some of the molecules found in the mycobacterial cell wall are also secreted into the biofilm matrix. Several components of the cell wall have also been linked directly to virulence.

As said, different mycobacteria have different lipids in the envelope. Glycopeptidolipids, which have been studied a lot, are found in *M. smegmatis* and *M. avium*, but not in *M. tuberculosis* or *M. marinum* [59, 69]. In *M. tuberculosis* the envelope contains phenolic glycolipids, phthiocerol dimycocerosate and lipooligosaccharides [69].

Lipoarabinomannan

Lipoarabinomannan is a glycophospholipid that is anchored to the mycobacterial plasma membrane, but also found in the upper layers of mycobacterial cell envelope [70]. All mycobacteria produce lipoarabinomannan, since it is a part of the characteristic mycobacterial cell wall structure [71]. Lipoarabinomannan binds to cell surface receptors of macrophages and dendritic cells inducing various immunomodulatory effects, downregulating the cell mediated immunity and aiding the invasion of the host cell [72].

Lipoarabinomannan is known to insert itself into the endomembranes and traffic within the infected cells. It is also known to inhibit the phagosomal maturation [70]. The lipoarabinomannan of *M. tuberculosis* is capped with mannose and it prevents the increase in Ca^{2+} levels during *M. tuberculosis* infection. The lipoarabinomannan found in non-pathogenic mycobacteria lacks the mannose cap and cannot cause this inhibition, suggesting that the mannose cap is essential for the inhibition [70]. Mannose also acts as a lipid anchor of lipomannan and lipoarabinomannan [73].

Another glycophospholipid, phosphatidylinositol mannoside, also plays a role in *M. tuberculosis* infection. Phosphatidylinositol mannoside promotes the fusion of early endosomal compartments while lipoarabinomannan prevents the attachment of late endosomal and lysosomal factors [70]. Together these effects prevent the phagosome maturation and fusion with the lysosome while helping the fusion of mycobacteria containing phagosomes.

Lipooligosaccharides

The lipooligosaccharides in *M. marinum* are required for sliding motility and entry to macrophages [68]. Defects in lipooligosaccharide biosynthesis also cause defects in biofilm formation [68]. The inefficient phagocytosis of the mutants suggests that the lipooligosaccharides interact directly with the host macrophages [68].

Lipooligosaccharides were originally found in *M. kansasii* [74], but they are also present in some *M. tuberculosis* and *M. marinum* strains [68]. In *M. kansasii* lipooligosaccharides are only found in smooth strains, but similar correlation between colony morphology and lipooligosaccharides has not been found in *M. tuberculosis* [75, 76]. The *M. kansasii* strains completely lacking the lipooligosaccharides cause chronic systemic infections in mice, but the smooth variants, which produce lipooligosaccharides, are cleared quickly from the animal's organs and fail to cause a proper infection [68]. It was therefore suggested that lipooligosaccharides might be an avirulence factor that somehow overcomes the effects of the other cell wall lipids. Most clinical isolates of *M. tuberculosis* do not contain lipooligosaccharides, supporting the previous idea [68]. However, in *M. marinum* lipooligosaccharides are required for phagocytosis, which invalidates the idea of lipooligosaccharides as an avirulence factor.

In *M. kansasii* there are eight closely related lipooligosaccharides. They all have the same tetraglucose structure: D-Glc*p*-($\beta 1 \rightarrow 3$)-D-Glc*p*-($\beta 1 \rightarrow 4$)-D-Glc*p*-($\alpha 1 \rightarrow 1\alpha$)-D-Glc*p*. This structure contains the trehalose moiety at the end [68]. All *M. kansasii* lipo-oligoaccharides also contain a 3-O-methylrhamnose and varying amounts of xylose, fucose and N-acylkansosamine, which is a novel N-acyl amino sugar. In other mycobacteria there are significant variations in both core sugar groups and in terminal sugar moieties [68]. Since lipooligosaccharides are located on the surface and there are significant variations in the terminal immunodominant monosaccharide between mycobacterial species, they can be used to serotype the particular mycobacterial species [68].

M. marinum produces four types of lipooligosaccharides, which are named LOS-I, LOS-II, LOS-III and LOS-IV. The core sugar groups are similar to *M. kansasii*, but the terminal sugar moieties are unique to allow the serotyping [77]. Disruption of the *losA* gene, which encodes a glycosyltransferase, prevents the formation of LOS-IV and causes accumulation of LOS-III, so the *losA* gene is part of the LOS-IV biosynthesis [77]. Also the lack of LOS-IV causes defects in macrophage entry [68]. Other genes related to the lipooligosaccharide synthesis in *M. marinum* have been identified. Disruption in gene *MM2309* prevents the synthesis of LOS-II and disruption in gene *MM2332* causes an intermediate of LOS-I and LOS-II to accumulate [68]. This intermediate lacks an unidentified sugar residue, suggesting that *MM2332* encodes an enzyme involved in the synthesis of the said sugar molecule or an enzyme responsible of the transfer of the sugar molecule [68]. These defects can be rescued with corresponding genes of the wild type *M. marinum*. Both of these mutations also cause altered colony morphology [68]. The gene *MM2309* encodes for UDP-glucose dehydrogenase, which converts UDP-D-glucose to UDP-D-glucuronate in the UDP-D-xylose synthesis. The *MM2310* gene, which is downstream from the *MM2309* gene most likely encodes UDP-glucuronate decarboxylase, which catalyzes the second step of UDP-D-xylose synthesis [68].

The genes *MM2309*, *MM2310* and *MM2332* are all found in the same genetic locus [68]. This locus containing genes *MM2309* through *MM2341* is considered as the lipooligosaccharide biosynthetic cluster. Other cell wall lipid biosynthesis genes are often organized in a similar fashion [68]. The genes *MM2309* through *MM2318* are in the same orientation, but only genes *MM2309* through *MM2312* were found to be transcribed together. The polycistronic operon containing these genes does not contain gene *MM2313* [68].

Phenolic glycolipids

Phenolic glycolipids have a long-chain fatty acid backbone consisting of *p*-glycosylated phenylglycols that have been diesterified with di- to tetramethyl branched acyl chains [78]. They are produced only by pathogenic mycobacteria and only by some clinical isolates of *M. tuberculosis* [78]. However, the *M. tuberculosis* strains producing phenolic gly-

copeptidolipids are hypervirulent and they inhibit the release of proinflammatory effector molecules [79]. It seems that the production of phenolic glycolipids correlates with the hypervirulence but does not cause it. *M. marinum* mutants lacking phenolic glycolipids have defects in cording and these mutants also have attenuated infection phenotypes in zebrafish [78]. The phenolic glycolipids are believed to inhibit the release of proinflammatory cytokines [13]. In *M. leprae* they are involved in attachment and entry to the Schwann cells [78].

The genes involved in the production of phenolphthiocerols, which is the backbone of phenolic glycolipids, come from the same gene cluster. This same gene cluster also produces the enzymes required for synthesis of phthiocerol dimycocerosate [78]. To produce phenolphthiocerol in *M. marinum* *p*-hydroxybenzoic acid is first converted to *p*-hydroxyphenylalkanoic acid, which is then converted to phenolphthiocerol. The mycocerosates are synthesized by a specific polyketide synthase, Mas or FadD28. The phenolphthiocerols are then diesterified with mycocerosates by PapA5 enzyme. The last step of production of phenolic glycolipids is the glycosylation [78]. The structures of phenolic glycolipids are similar in *M. marinum* and *M. tuberculosis*, but the stereochemistry of their mycocerosates is different. In *M. marinum* the mycocerosates are dextrorotatory, while in *M. tuberculosis* they are levorotatory [78]. It would be interesting to know whether the *M. marinum* Mas enzyme could be replaced with the corresponding enzyme from *M. tuberculosis* and if it could, how the different stereochemistry would affect the structure of the cell envelope or the biofilm.

Phthiocerol dimycocerosate

Phthiocerol dimycocerosates have been identified in several pathogenic mycobacteria, including *M. marinum* and *M. tuberculosis* [78]. In *M. tuberculosis* the phthiocerol dimycocerosates prevent the phagosomal maturation. The *M. marinum* and *M. tuberculosis* strains with impaired phthiocerol dimycocerosate production or localization cause attenuated infections in animal models [8, 78]. In *M. marinum* the lack of phthiocerol dimycocerosate causes visible defects in cording and reduces virulence [78]. In both *M. tuberculosis* and *M. marinum* lacking phthiocerol dimycocerosates or phenolic glycolipids, the cell wall becomes more permeable and the bacteria are more susceptible to antibiotics [78]. Phthiocerol dimycocerosates are therefore important for both virulence and for the cell wall structure, and therefore for the biofilm as well.

Phthiocerol dimycocerosate backbone consists of 3-methoxy (or 3-keto, 3-hydroxy), 4-methyl, 9,11-dihydroxy glycols, which are then diesterified similarly as phenolic glycolipids. In *M. marinum* many of the genes used for synthesis of are similar or same as the ones used in the phenolic glycolipid synthesis [78]. All the genes come from the same gene cluster, both the genes for synthesis of phthiocerol dimycocerosates and for the synthesis of phenolic glycolipids. The mycocerosate is produced by the same enzymes,

Mas or FadD28. Also the enzyme that catalyzes the diesterification of phthiocerols and mycocerosates is the same one that catalyzes the diesterification of phenolphthiocerols and mycocerosates [78].

The stereochemistry of mycocerosates affects also phthiocerol dimycocerosates. It seems possible that the enzymes could be substituted with each other, but it would certainly affect the structure of the cell envelope, since it would be more than one kind of lipids that would be affected. Since the integrity of the cell wall is essential for the proper biofilm formation, this wide changes in the structure of the envelope would certainly affect the biofilm formation.

2.5.3 Extracellular matrix of mycobacterial biofilms

The extracellular matrix (ECM) in other biofilm forming bacteria consists most often of exopolysaccharides, proteins and DNA [54]. Exopolysaccharides are one of the most predominant components of biofilms in Gram-positive and Gram-negative bacteria [80]. Mycobacterial biofilms are exceptional, since mycobacteria do not secrete polysaccharides and it seems that they are not even able to produce them [54]. Another important component of the ECM in many bacteria, including mycobacteria, is extracellular DNA (eDNA). The ECM also contains some proteins, which are related especially to the cell to cell and cell to surface attachment [6]. The composition of the ECM varies a lot between different species and even strains. The ECM holds the bacteria residing in the biofilm together [6].

The ECM of mycobacterial biofilms is very lipid rich. Some of the lipids present in the cell envelope are also secreted to the ECM and sometimes the cell envelope is considered as part of the ECM. The lipids facilitate the attachment of the biofilm to surfaces by creating a hydrophobic outer surface [60]. Since mycolic acids seem to be essential at least for *M. smegmatis* biofilms, they will be discussed in more detail in the following section [5]. After that extracellular DNA will be discussed as a component of the ECM, since it too seems to be important for mycobacterial biofilms.

Mycolic acids

Mycolic acids are long-chain fatty acids (C_{70}-C_{90}) and they are part of the charasteristic mycobacterial cell wall [5, 54]. The general structure of all mycobacterial mycolic acids contains a C_{26} fatty acid chain, which is condensed with a longer and more variable fatty acid [54]. Mycolic acids in mycobacterial cell walls are bound to arabinogalactan polysaccharide layer, which is linked to the peptidoglycan layer [60]. These were the first to be the only mycolic acids present in mycobacterial biofilms. However, mycolic acids are also secreted by mycobacteria and they are present in biofilms also extracellularly. The secreted ones are referred to as free mycolic acids [81]. For example *M. tuberculosis*

biofilms are rich in extracellular free mycolic acids [3]. Changes in the environmental conditions affect the structures of mycolic acids. *M. smegmatis* residing in biofilms produces shorter ((C_{56}-C_{68})) mycolic acids than the planktonic bacteria [5].

The synthesis of mycolates, which are the esters of mycolic acids found in the mycobacterial cell wall, is modulated by GroEl1 [5]. The *M. tuberculosis* mutants with defects in mycolate synthesis have attenuated phenotypes. Short-chain mycolates are upregulated during biofilm formation [5]. GroEL1 associates with KasA, which is also involved in the synthesis of mycolic acids. Biofilm formation is linked to higher production of short-chain fatty acids [5].

Mycobacteria have two GroEL paralogs. GroEL2 is essential for survival and it has a more typical chaperone structure with a glycine-methionine-rich C-terminus. GroEL1 on the other hand has a histidine rich C-terminus and it is not required for cell survival [5]. Similar GroEL1 has also been found in *Corynebacterium* and *Nocardia* and they also have mycolic acids in their cell walls so it is possible that they have similar regulation of mycolic acids biosynthesis [5]. In *M. tuberculosis* both of these GroEL paralogs are induced during heat shock, oxidative stress response and macrophage infection [5].If biofilm formation is a typical stress response of mycobacteria, then the upregulation of these genes could be linked to biofilm formation. Loss of *GroEL1* in *M. smegmatis* does not affect planktonic cells or surface attachment, but it prevents the biofilm maturation [5].

KasB is only required to add the last ethyl group to mycolic acids in mycobacteria. *KasA*, which associates with GroEl1, is a close homologue of *kasB*. Both *kasA* and *kasB* are conserved in *M. marinum* and *M. tuberculosis* and their functions are also conserved [36]. In *M. marinum* mutation in *kasB* grow poorly in macrophages, but normally *in vitro*. The mycolic acids produced by these mutants are 2 to 4 carbons shorter and the levels of keto-mycolates are reduced [66]. Even though these changes are small, they increase the cell wall permeability massively leading to higher susceptibility to lipophilic antibiotics as well as the host immune system. The more permeable cell wall allows host's lysozyme enter the bacterial cells [66]. The mutants are also unable to form cords. These defects can be rescued with *M. tuberculosis kasB*, but not with *kasA*. Expression of *kasA* slows down the growth rate in both liquid medium and on agar [66]. Corresponding mutation in *M. tuberculosis kasB* causes similar alterations in the cell wall and a significantly attenuated infection in mice [82].

Free mycolic acids are an abundant component of the *M. smegmatis* biofilms in the later stages of the bacterial growth [81]. They are also abundant in *M. tuberculosis* pellicles [3]. However, the free mycolic acids found in *M. smegmatis* and *M. tuberculosis* biofilms are structurally different, even though the biofilms appear morphologically similar [6]. Since certain components of biofilms are linked to pathogenicity, it is possible that these structural differences in free mycolic acids affect the difference in virulence between *M. smegmatis*, which is not pathogenic, and *M. tuberculosis*, which is highly

pathogenic. On the other hand, purified free mycolic acids from *M. tuberculosis* do not induce a proinflammatory response in macrophages [6], suggesting that free mycolic acids do not interact directly with macrophages or the response requires another component.

Trehalose dimycolate

In detergent free *in vitro* cultures *M. tuberculosis* forms cord structures. The cords are rich in trehalose dimycolate, which is an extracellular glycolipid found in mycobacterial biofilms [81]. This glycolipid induces granuloma formation in animal models and mutants with defects in cording are unable to cause a chronic and lethal infection, even though the initial replication is normal [83]. Disruption of trehalose dimycolate synthesis causes severe defects in biofilm development in *M. smegmatis*. Similar effects are most likely seen in*M. tuberculosis*, since trehalose dimycolate is the precursor of mycolic acids and the pathways of mycolic acid synthesis are closely related between *M. smegmatis* and *M. tuberculosis* [81]. Trehalose dimycolate is required for cording and normal pathogenesis in *M. tuberculosis*, but mutants with low levels of trehalose dimycolate can still survive. In *M. smegmatis* the drug tolerance correlates with induced synthesis of free mycolic acids [81].

Trehalose dimycolate is the precursor of free mycolic acids, but only newly synthesized trehalose dimycolate can be used as a precursor [81]. This is most likely due to cellular localization. The enzyme responsible for production of free mycolic acids is hypothesized to be located in the periplasmic space between the inner and outer membranes. The enzyme can only convert molecules located in the same cellular location and the preexisting trehalose dimycolate is integrated into the outer cell wall [81]. Also the free mycolic acids are produced by other pathways as well since disruption of the trehalose dimycolate synthesis only reduces the levels of free mycolic acids [81]. The existence of several production pathways is often an indication that the particular molecule is important for the cell's survival.

Extracellular DNA

Extracellular DNA (eDNA) is an found in many non-mycobacterial biofilms [63]. It was first reported by Whitchurch *et al.* [84] in *Pseudomonas aeruginosa* biofilms. In other bacteria eDNA has several important roles [63]. In *P. aeruginosa* it is known to facilitate cellular aggregation [85] and spatial self-organization [86]. eDNA can also be transferred horizontally [87]. The horizontal transfer could be used to spread antibiotic resistance within the biofilm. In *Vibrio cholerae* eDNA contributes to nutrient acquisition, biofilm architecture, detachment from the biofilm and colonization in the new location [88]. Since eDNA helps to hold the biofilm structure together, it also protects the bacteria residing in within the biofilm from antibiotics and detergents.

It is not yet known how eDNA is generated. The eDNA production mechanisms can be divided to two groups; cell lysis dependent and cell lysis independent mechanisms. In cell lysis dependent pathways some of the bacteria sacrifice themselves for the benefit of the colony. This has been shown in *P. aeruginosa* biofilms, where the cell lysis dependent eDNA production is prophage-mediated and controlled by quorum sensing [89]. In both *P. aeruginosa* and *M. avium* subsp. *hominissuis* the eDNA was found to be similar to the genomic DNA, supporting the theory of cell lysis dependent eDNA production [63,89]. If the eDNA production pathway s independent of cell lysis, the eDNA has to be transported to matrix. there are several studies also supporting these mechanisms [63]. Most likely the production pathway depends on the bacterial species and on the growth conditions.

Distinct wrinkling appearance of mycobacterial biofilm has been linked to greater eDNA production [63]. In *Bacillus subtilis* biofilms the wrinkling pattern was linked to cell death [90]. Cell death would release eDNA into the biofilm and therefore there might also be a link between wrinkled structure and eDNA in *B. subtilis* biofilms. *M. marinum* produces little eDNA when compared to other non-tuberculous mycobacterial strains [63]. At least in *M. avium* subsp. *hominissuis* the amount of eDNA is not directly proportional to bacterial count, since the bacterial count did not vary a lot between day 1 and day 7, but the amount of eDNA had increased massively [63]. Possibly each lysed bacteria contributes their genomic DNA to the biofilm matrix and as time passes the eDNA is not degraded but accumulates. The bacterial count has a limit set by the growth conditions, but most likely the eDNA does not have a maximum limit as long as the biofilm colony is functional.

Since DNase is known to disrupt biofilms, it could be combined with antibiotics to improve their effectiveness when treating mycobacterial infections. An inhaled DNase adjuvant has already been approved for treatment of cystic fibrosis [63].

2.6 MycoMar T7

MycoMar T7 is a mariner-based transposon system and it contains T7 promoters promoting the transcription of the adjacent chromosomal DNA [91]. The transposon is flanked by 29 base pair repeats and the T7 promoters are recognized by T7 RNA polymerase, which is a very active enzyme [92,93]. Therefore the phage can both interrupt the coding sequence and induce overexpression of the adjacent DNA segment. The result depends on the insertion site. MycoMar T7 integrates to the genome randomly.

The phage is designed to lyse mycobacteria at around 30 °C and integrate at 37 °C. It contains the kanamycin resistance gene as a selection marker. Kanamycin, hygromycin and streptomycin are the most commonly used antibiotics as selection markers in mycobacteria [8]. Kanamycin is often favored because of its high stability and low cost. Spontaneous mutations resulting in kanamycin resistance are also quite rare in *M. smegmatis*, which is often used due to its short generation time [8].

3. MATERIALS AND METHODS

In this experiment several screens were conducted in order to find biofilm mutant *M. marinum* strains. Eventually six mutants were chosen and their growth rates were determined. The phage stock preparation and transduction protocol were adapted from Murry *et al*. 2008 [94]. The MycoMar T7 phage used for transductions was received from Eric Rubin Lab, Harvard.

3.1 Phage stock preparation

Mycobacterium smegmatis ATCC-700084 (ATCC, U.S.) was grown on a LB plate at 37 °C for several days. The LB plate was prepared from LB broth with agar (Sigma-Aldrich, U.S.), which was dissolved in sterile H_2O according to instructions. *M. smegmatis* was then inoculated from the plate to 1.5 ml of Difco Middlebrook 7H9 broth (BD, U.S.) growth medium as triplicates. The 7H9 growth medium contained 0.4 % of glycerol, 10 % of Middlebrook ADC enrichment (BD, U.S.) and 0.05 % of Tween®80 (Sigma-Aldrich, U.S.) dissolved in sterile H_2O. The *M. smegmatis* cultures were grown for 24 hours at 37 °C and 225 rpm on a CERTOMAT® RM shaker (B. Braun Biotech International, Germany) after which one of them was chosen for further dilution. 10, 15 and 20 μl of the chosen *M. smegmatis* culture was diluted to 10 ml of the 7H9 growth medium. These were grown for 24 h at 37 °C and 225 rpm on a shaker before washing and plating.

10-fold dilutions of the MycoMar T7 phage were prepared to a volume of 50 μl of MP buffer. MP buffer contained 50 mM Tris-HCl, 150 mM NaCl, 10 mM $MgSO_4$ and 2 mM $CaCl_2$ dissolved in sterile H_2O. The absorbance at 600 nm was measured from the *M. smegmatis* cultures and a culture with absorbance between 0.8 and 1.2 was chosen. This culture was then washed twice with MP buffer and with centrifuge settings of 3 min at 10 000 g. After the second wash *M. smegmatis* was concentrated according to formula:

$$concentrationfactor = \frac{3.2}{OD_{600}}, \tag{3.1}$$

where OD_{600} is the absorbance at 600 nm. The formula is derived from empirical experience of Hammarén, M., University of Tampere.

100 μl of the concentrated *M. smegmatis* culture was mixed gently with each of the 50 μl phage dilutions. Each mixture was mixed with 3.5 ml of top agar and poured on a

15 cm LB plate. The top agar contained 0.6 % (w/v) of low gelling temperature agarose (Sigma-Aldrich, U.S.) and 2 mM of $CaCl_2$ in 7H9 broth with 0.4 % of glycerol but without Tween®80 and enrichment. The plates were incubated for 2 days at 29 °C.

Another set of LB plates containing *M. smegmatis* in top agar were prepared, but these plates did not contain the phage. Several plaques were patched to these new plates by touching the plaque with a pipet tip, then pipetting back and forth in 50 μl of MP buffer. Then a 10 ul drop was pipetted onto the plate. This was repeated for 9 plaques. Two identical LB plates were prepared in this manner. One was incubated at 29 °C and the other at 37 °C for 2 days.

A clone which formed plaques only at 29 °C was chosen and excised from agar with a sterile blade. The excised agar was incubated in MP buffer at 4 °C for 2 hours after which the agar was crushed and centrifuged at 200 g for 2 min. The supernatant containing the phage was collected and 10-fold dilutions were made from it. These dilutions were then mixed with *M. smegmatis* and plated in top agar as previously. The plates were incubated at 29 °C for 2 days. A dilution with nearly confluent plaques was chosen for phage production.

Seven plates with the chosen dilution were prepared as previously, but this time LB plates were not used. Instead the plates were prepared from Difco Middlebrook 7H10 (BD, U.S.) with 5 % of glycerol and 10 % of Middlebrook OADC enrichment (BD, U.S.). The plates were incubated at 29 °C for 2 days. Each plate was flooded with 3 ml of MP buffer and the plates were rocked gently for 24 hours at 4 °C. The MP buffer was collected from the plates and passed through 0.2 μm syringe filter. This phage stock was titered by pipetting 10 μl drops of 10-fold dilutions as triplicates on a plate containing *M. smegmatis* in top agar as previously described. The plate was incubated at 29° C for 2 days after which the formed plaques were counted to determine the concentration of the stock.

3.2 Transduction

The concentration of the kanamycin for the transducts was determined by plating two different concentrations of *Mycobacterium marinum* ATCC927 (ATCC, U.S.) on plates with different antibiotic concentrations. The bacterial concentrations were calculated to be around 10 and 100 cfu/μl with plating volume of 100 μl. The plates with kanamycin concentrations of 25, 40 and 50 μg/ml were prepared by absorption on 85 mm plates and one 150 mm plate was prepared by adding 25 μg/ml of kanamycin to agar before pouring onto plates. Controls without antibiotic were also prepared for each bacterial concentration.

M. marinum was grown in 7H9 broth containing 10 % OADC and 0.05 % Tween®80 until absorbance at 600 nm was between 0.8 and 1.0. The *M. marinum* culture was washed twice with MP buffer and centrifuged at 10 000 g for 3 min. Then the pelleted culture was

resuspended in adsorption buffer. The adsorption buffer was prepared from Difco Middlebrook 7H9 broth according to instructions, but there was only and 0.02 % of glycerol and no enrichment. 1 ml aliquot was removed to serve as a wild-type control. 10-fold amount of phage was added to *M. marinum* for transduction and MP buffer was added to the control in the same volume to volume ratio. The mixtures were incubated at 37 °C for 3 h. Tween®80 was added to the concentration of 0.05 % and the mixtures were incubated for 30 min at 29 °C. The transduction mixture was divided into aliquots of 2 ml, which were concentrated to half of the volume and stored at -80 °C. To determine the correct dilution for the desired plating density the transducts were titered as 10-fold dilutions on 7H10 plates containing 50 μg/ml kanamycin. These plates were incubated at 29 °C for 7 days.

The transducts were plated in the chosen dilution on 7H10 plates containing 50 μg/ml kanamycin and incubated at 29 °C for 2 weeks. Small single colonies were picked at different time points during the second week to 96 well plates containing 7H9 broth with 0.05 % of Tween®80, 0.4 % of glycerol and 50 μg/ml of kanamycin. The 96 well plates were incubated at 29 °C for a week and then stored at 4 °C.

3.3 First and second screens

For the first screen the transduct colonies were transferred by pipetting 5 μl from each well of the original 96-well plate set to a corresponding well in the second set of 96-well plates containing 0.2 ml of biofilm medium. The biofilm medium had a 7H9 broth base, and it contained 0.05 % Tween®80, 0.4 % glycerol and 5 % of OADC enrichment. The wild-type *M. marinum* control prepared alongside the transduction was used as a control. The plates were wrapped in parafilm and incubated at 29 °C for 5 weeks. Once a week the plates were viewed with a Zeiss Stemi 2000 microscope (Zeiss, Germany) to distinguish the mutants with seemingly different biofilm production. The differences in the biofilm formation were approximated and the ones unable to form the pellicle or with otherwise abnormal biofilm structure were chosen for the second screen.

For the second screen 100 μl of the chosen mutants were taken from the original 96-well plates and diluted to 4 ml of biofilm medium in cell culture tubes. One control tube with wild-type *M. marinum* was also prepared. The cultures were incubated at 29 °C with closed caps. The growth was monitored during the first month of incubation. The cultures were stored at the incubator. The transducts that had grown clearly visible biofilms were chosen for the third screen. The other mutants chosen for the second screen most likely had some growth defects induced by the transposon.

Table 3.1: The sequences of the MMITS1 primers.

Primer	Sequence
Forward	5'-CACCACGAGAAACACTCCAA-3'
Reverse	5'-ACATCCCGAAACCAACAGAG-3'

3.4 Colony qPCR

The species of the mutants was verified with qPCR, since the abnormal biofilm could also be a sign of a strong contamination. *M. marinum* specific primers were used. These primers are designed to pair only with *M. marinum* DNA and their sequences are presented in 3.1. The primers were diluted from stock to concentrations of 10 μM.

A fresher *M. marinum* culture was prepared for control. *M. marinum* was streaked from the 7H10 plate to 10 ml of 7H9 broth with ADC enrichment and 0.05 % Tween®80. The culture was incubated at 29 °C and three days later it was diluted so that the absorbance at 600 nm was 0.07. The diluted culture was incubated at 29 °C for a week. This culture was used in the qPCR also as a 1:10 dilution.

The reaction mixture of the qPCR is presented in table 3.2. A master mix containing everything but the sample was prepared and pipetted on a 96-well plate. Sterile water was used as a negative control. The fresher *M. marinum* culture was used as a species reference control and the species of the older wild-type control was also determined in a similar fashion as the mutants. Two replicates were prepared from all samples and controls. The samples were added by pipetting 1 μl from the culture directly to the well containing the qPCR mixture. The plate was sealed with a transparent film and centrifuged for 2 min at 2 000 g and 4 °C. The program is presented in table 3.3 and it was run on BIO-RAD CFX96 cycler. The standard deviations for threshold cycles were calculated with Microsoft Excel.

Table 3.2: The reaction mixtures of colony qPCR and bacterial count determination. The arrows represent forward and reverse primers.

Component	Colony qPCR (μl)	qPCR for bacterial count (μl)
Sensifast NO-ROX SYBR, Green Master Mix	10	10
Primer MMITS1 $\rightarrow$	0.8	0.8
Primer MMITS1 $\leftarrow$	0.8	0.8
Sterile H_2O	7.4	5.4
Sample	1	3
Total volume	20	20

Table 3.3: The program for qPCR. The melting curve analysis at the last step was measured between 55 and 95 °C with 0.5 °C intervals.

Step	Time	Temperature	Fluorescence detection
1	3 min	95 °C	
2	5 s	95 °C	
3	10 s	65 °C	
4	5 s	72 °C	Yes
5	Go to 2 39 times		
6	Melting curve analysis		

3.5 Third screen

The cultures for the third screen were prepared and incubated in a similar fashion as the cultures in the second screen. 100 μl of the second screen culture was diluted to 4 ml of biofilm medium containing 50 μg/ml of kanamycin. The wild-type control was grown without kanamycin. Due to the seemingly slow growth rate of the mutants, seven replicates were prepared of each mutant and also of the control. One set of all mutants and the control was also prepared in the richer 7H9 broth containing 10 % of ADC enrichment. The cultures were incubated at 29 °C with caps closed. After six week incubation one culture tube of each mutant and the control was used for analysis. The culture was homogenized, 1 ml was taken for the crystal violet staining, 2 ml for qPCR and 0.5 ml for DNase treatment. The aliquots were stored at 4 °C.

Crystal violet staining

The crystal violet protocol was adapted from Carter *et al.* 2003 [59]. The 1 ml samples were centrifuged at 10 000 g for 3 min and the supernatant was removed. The pellet was resuspended in 1 ml of Gram's Crystal Violet Solution (Sigma-Aldrich, U.S.) and incubated for 15 min. Then the samples were centrifuged again with same settings and the crystal violet solution was removed. The samples were then washed four times with purified water. After the fourth wash the sample was resuspended in 95 % ethanol and incubated for 10 min. The cell debris was centrifuged to the bottom and 200 μl of the ethanol solution was pipetted on a 96-well plate as two replicates. The absorbance was measured at 600 nm with EnVision 2104 Multilabel Reader (PerkinElmer, U.S.).

Standard curve

A standard was prepared for qPCR to determine the bacterial count. *M. marinum* was grown in 7H9 broth containing 0.05 % of Tween®80 for two days at 29 °C. The absorbance was measured at 600 nm and the bacterial count approximated from it according

to formula:

$$CFU/\mu\text{l} = 276165 * OD_{600}^2 - 2470.7 * OD_{600} + 21389, \quad (3.2)$$

where OD_{600} is the absorbance at 600 nm. The equation is from the Master's thesis of Milka Hammarén [95]. 2 ml of the culture was then pelleted and frozen at -80 °C.

DNA isolation and qPCR

2 ml aliquots of the mutants were pelleted, the supernatants removed and the pellets was frozen at -80 °C. The frozen mutant pellets and the standard curve pellet were then resuspended in 1.5 ml of TRI reagent for DNA-RNA co-extraction (MRC, USA) and homogenized with PowerLyzer24 bead beater (Mobio, USA) in three 20 s cycles at 3 200 rpmi with 30 s pauses in between. Then the samples were sonicated in an m08 water bath (FinnSonic, Finland) for 9 min and centrifuged at 4 °C 12 000 g for 10 min. 1 ml of the homogenate was taken, RNA was removed according to the manufacturer's protocol and the DNA was extracted according to the manufacturer's alternative protocol. The purified DNA was resuspended in 50 μl of nuclease free water. The DNA concentrations were measured with NanoDrop 2000 (Thermo Scientific, U.S.). The standard curve was prepared by diluting the purified standard DNA in ten-fold dilutions. The bacterial counts were then determined with qPCR with the same protocol as described for colony qPCR and the standard curve as reference. The Bio-Rad CFX Manager was used to determine the bacterial concentrations of the mutant samples based on the standard curve.

DNase treatment

The 500 μl taken for the DNase treatment was centrifuged at 10 000 g for 3 min and the pellet was resuspended in 400 μl of DNase I buffer containing 2.5 mM of $MgCl_2$. The amount of DNase I (Thermo Scientific, U.S.) was approximated based on the qPCR results of the previously run samples and the size of the *M. marinum* genome according to the formula:

$$V_{DNase\ I} = \frac{CFU * N_{Mm}}{1000 * N_{pg}} * V_{sample}, \quad (3.3)$$

where $V_{DNase\ I}$ is the amount of DNase I needed (μl), CFU is the bacterial count according to the qPCR (CFU/μl), N_{Mm} is the number of base pairs in *M. marinum* genome, N_{pg} is the number of base pairs in 1 pg of DNA and V_{sample} is the volume of the sample (ml). The amount of basepairs in *M. marinum* genome is 6 636 827 bp [96] and 1 pg of DNA contains 978 Mbp [97]. The results were rounded up to the next full μl. Since the wild-type required significantly larger volume of the enzyme, the DNase I buffer was added as more concentrated so the DNase I would dilute it to the correct concentration. The bacteria were incubated with DNase I for 2 h at 37 °C after which the DNase I was

inactivated at 70 °C for 10 min. The samples were pelleted, the supernatant was removed and the pellets were stored at -80 °C. The DNA was extracted as previously, except the purified DNA was diluted to 25 μl of nuclease free water. The bacterial concentrations of the DNase I treated samples were analyzed with qPCR as previously described.

Protocol alterations for the second time point

The crystal violet staining, DNase I treatment and the qPCR analysis was repeated for another set of tubes after 8 week incubation. The same protocol was followed with a few exceptions. In the crystal violet assay a ten-fold dilution was prepared from the ethanol solution of wild-type control and the absorbance was also measured from this dilution. The qPCR analysis was conducted for all the samples at the same time, so the amount of DNase I added to the samples was based on the previous results and therefore the added volumes were exactly the same as previously. Also the samples were centrifuged and the supernatant was removed before the DNase I was inactivated.

Analysis of the results

The results were analyzed on Microsoft Excel. A concentration factor was calculated for all DNA extractions by formula:

$$CF = \frac{V_{sample}}{V_{DNA}}, \tag{3.4}$$

where CF is concentration factor, V_{sample} is the volume taken from the culture and V_{DNA} is the volume where purified DNA was resuspended. The concentration factor was compared to the one calculated for the standard curve and the starting quantity received from the Bio-Rad CFX Manager was adjusted accordingly to get the bacterial count of the original culture.

The amount of biomass per bacteria was calculated with formula:

$$biomass/bacteria = \frac{CV}{bacterial\ count}, \tag{3.5}$$

where CV is the absorbance measured in the crystal violet assay and bacterial count is the bacterial count of the original culture calculated from the DNase I treated samples. The amount of eDNA/bacteria was calculated with formula:

$$eDNA/bacteria = \frac{DNA_{ALL}}{bacterial\ count} - 1, \tag{3.6}$$

where DNA_{ALL} is the bacterial count received from the sample not treated with DNase I and the bacterial count is the bacterial count of the original culture.

3.6 Glycerol stock preparation

The mutants and the control prepared alongside transduction were grown at 29 °C on 24-well plates in 1 ml of 7H9 broth containing 10 % of ADC enrichment and 0.05 % of Tween®80 for 1 week. Images were taken f the wells before the stocks were prepared. Each well was homogenized and diluted to half with 40 % glycerol solution. The diluted glycerol cultures were stored in -80 °C.

3.7 Growth rate and growth curves

Pre-cultures of the mutants and the control were prepared by streaking bacteria from a 7H10 plate to 9 ml of 7H9 broth containing 0.05 % of Tween®80. The pre-cultures were incubated at 29 °C for 3 days. On the third day the cultures were let to settle for 10 min and 5 ml of the top phase was taken. The pre-culture was added to cell culture tubes containing 5 ml of the same 7H9 broth until the absorbance at 600 nm of this prepared culture was 0.07. Three replicates of each mutant and the control were prepared. The cultures were incubated at 29 °C for 5 days. Each day the absorbance at 600 nm was measured and three different ten-fold dilutions of each tube were plated. The cultures were mixed properly before the absorbance was measured. The plated dilutions ranged from $1{:}10^2$ to $1{:}10^5$. The plated volume of each dilution was 10 μl.

A set of bottle cultures was also prepared from the same pre-cultures. The pre-culture was diluted to 9 ml of the same 7H9 broth to reach 0.07 absorbance at 600 nm. These cultures were grown in cell culture bottles at 29 °C for 4 days. Then the cultures were settled for 10 min and 5 ml of the top phase was collected. The absorbance was measured from the top phase and then ten-fold dilutions were plated similarly as from the tube cultures. The plates from both tube and bottle cultures were counted 4 days after plating.

The growth rates were determined based on the results of three days growth in cell culture tubes. The smallest dilutions with separate colonies on the plate was used as a basis for the bacterial count calculations. The absorbance values and the bacterial counts were plotted to graphs on Microsoft Excel. The software was used to draw linear trendlines and determine their slopes. The correlations between the absorbance values and the bacterial counts were also calculated. When the cultures tubes and bottles were compared to one another, the ratio between the optical density and the bacterial count was calculated for each culture tube separately and then average was taken from these results.

4. RESULTS AND DISCUSSION

In this chapter the results are presented and discussed in the order in which they were obtained. Therefore the chapter follows the same order of presentation as the previous chapter.

4.1 Phage stock preparation and transduction

The phage production was conducted in *M. smegmatis* due to its faster growth rate and lower pathogenicity when compared to *M. marinum*. The concentration of the kanamycin had to be adjusted since there was growth on the control plates containing kanamycin and the wild-type *M. marinum*. Clean control plates were achieved with concentration of 50 μg/ml. The kanamycin seemed to also work better when it was absorbed to the plate instead of mixing it with the 7H10 solution before the plates were poured. The kanamycin was possibly sensitive to high temperature or it did not mix properly with the agar solution. By absorbing the kanamycin to plates the concentrations are most likely higher closer to the agar surface and lower at the bottom. The same concentration was used throughout the experiment with both liquid and agar cultures.

For plating of the transducted mutants a dilution of 1:100 was chosen. This concentration gave enough colonies on the plate, but the colonies remained mainly separate. The more diluted plate cultures grew barely at all, suggesting a possible link to quorum sensing.

There is no approximation in the literature about how many of the *M. marinum* genes are related to the biofilm formation. As described in chapter 2, the biofilm formation in *M. marinum* is a complicated process involving several metabolic pathways, which is also reflected in the amount of different components found in these biofilms. There are over 5 400 predicted coding sequences in the *M. marinum* genome [48]. We could assume that 20 % of these genes affect the appearance of the biofilm. Even though the insertion of the MycoMar T7 is random, there may still be some hotspots for the insertion, which would lead to mutant strains with similar or same mutations. Since there was no knowledge about the actual number of biofilm related genes nor about the insertion hotspots, 3 500 separate colonies were picked from the plates to ensure there would be at least a few different biofilm mutants.

It was hypothesized that mutant strains with biofilm defects would be smaller, since they form less matrix around them and the small size would mean they became visible

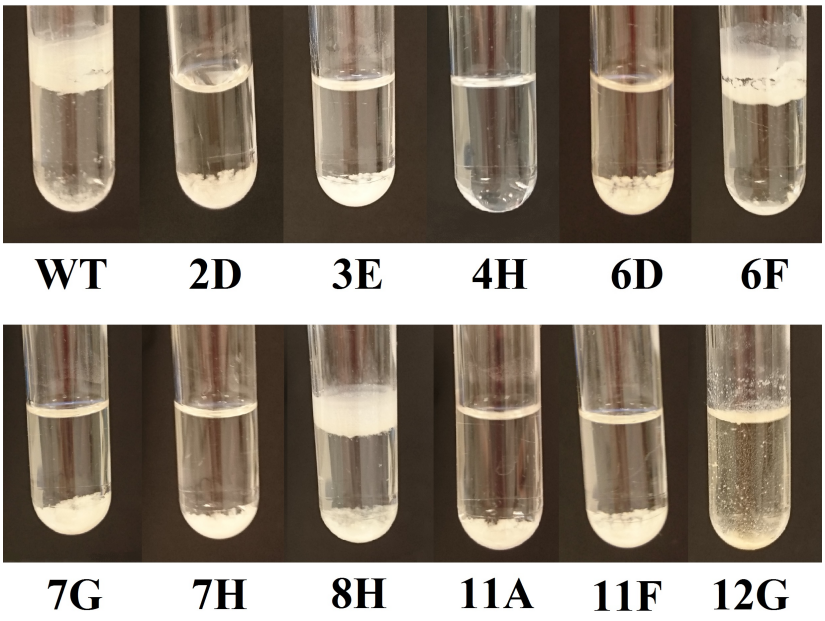

Figure 4.1: All the biofilm producing cultures from the second screen. 4H is an example of the non-growing mutants. WT stands for wild-type.

slightly later than others. Therefore the colonies were picked 10 days after plating and the picked colonies were all relative small.

4.2 First and second screens

In the first screen only around one tenth of the mutants grew at all. This is a very low percentage and suggests some kind of systematic error. The most likely explanation is that the small colonies that were picked from the plates had growth defects caused by the random mutation and they were therefore unable to grow in the biofilm medium, which had fewer nutrients than the typical growth media. 58 mutants with seemingly abnormal biofilms were chosen for the second screen.

In the second screen once again most of the mutants did not grow at all. Ten out of 58 mutants produced visible biofilms and these biofilms and the control are shown in figure 4.1. The figure also shows one of the mutants that did not grow at all in this screen. The mutants that produced biofilm had produced visible biofilms already after one month. The incubation was continued even after this hoping some of the other mutants would grow visible biofilms as well, but they did not.

One of the mutants, 12G, had a different coloration and the structure of its biofilm was also visibly different. The mutant was suspected to be contamination instead of *M. marinum*. The colony qPCR was used to find out whether there indeed was *M. marinum* present in the cultures or if the growth was mainly contamination.

Table 4.1: The means of the threshold cycles and the standard deviations from the colony qPCR. WT stands for fresh wild-type *M. marinum* culture, WT 1:10 for a 1:10 dilution of the same culture and WT CTRL for the wild-type control grown alongside the mutants.

Sample	Mean of the threshold cycles	Standard deviation
WT	20.53	0.06
WT 1:10	22.68	0.03
WT CTRL	15.43	0.67
2D	14.92	0.40
3E	14.67	0.13
6D	14.32	0.08
6F	16.67	0.48
7G	15.03	0.19
7H	4.72	0.38
8H	10.12	6.60
11A	14.70	0.16
11F	10.69	6.59
12G	36.16	0.02

4.3 Colony qPCR

The primers used in all qPCR assays were designed for the M. marinum 16S-23S ITS sequence [28]. They are supposed to recognize only *M. marinum* DNA. All *M. marinum* bacteria should have the same number of copies of the 16S-23S ITS sequence and therefore it can be used to quantify the number of bacteria present in the sample. The threshold cycles can be used to approximate the number of bacteria in the sample and low threshold cycles stand for high number of *M. marinum* DNA. However, in this colony qPCR the sample was not homogenized nor the DNA purified, so the amounts of accessible template are different in all samples and due to the uneven distribution of the template, the results cannot be used to quantify the bacterial count. However, low threshold cycles still suggest high *M. marinum* content. The threshold cycles of the colony qPCR are presented in table 4.1.

As can be seen from the table 4.1, some of the standard deviations are quite high, which is the result of the differences in the amounts of template. Interestingly, almost all the samples have lower threshold cycles than the fresh *M. marinum* controls. This high amounts of *M. marinum* DNA show that the biofilm present in the culture is in fact *M. marinum*. These results do not, however, rule out that there is some contamination growing alongside the *M. marinum*. Only the mutant sample 12G has higher threshold cycles than the *M. marinum* controls. This is the same mutant that was suspected to be contamination and these threshold cycles support that hypothesis. The sample 12G was therefore left out from the third screen.

4.4 Third screen

In order to determine, which mutant strains form abnormal biofilms, the amount of biofilm per bacterium needed to be quantified. Absorbance could have been used, but since it was likely that the mutants have different growth rates, there would have been a lot of variation in the bacterial counts. Absorbance is also quite unreliable in low-Tween®80 cultures, since the bacteria form clumps and the culture is not homogenic. Crystal violet staining is often used for biofilm quantification, but the problem with this method is that it does not stain only the matrix but also living and dead cells [98]. Therefore the stain was used to quantify the biomass and the results were then normalized with the determined bacterial count. Since the mutants had previously grown poorly on agar, qPCR was chosen as the method to quantify the bacterial count.

The protocol for the DNase I inactivation was altered for the second time point. The samples were centrifuged down and the supernatant removed before the DNase I was inactivated. The inactivation temperature was so high that it most likely disrupted some of the *M. marinum* cells. When the cells were centrifuged afterwards some of the intracellular DNA may have been removed in the supernatant. Though the exact results are not comparable between the two time points due to slightly different protocols, the mutants can be organized based on the results and these organizations can be compared between the two time points. Also the reference culture used for the standard curve most likely contained significantly less dead bacteria, since it was a lot fresher. If mycobacteria incorporates the DNA released from the dead bacteria to the biofilm as eDNA, then this fresher culture should have remarkably less eDNA and therefore the bacterial count would most likely be higher in the samples that have been incubated for a longer time. The bacterial counts are not therefore very reliable, but the standard curve allows the two different time points to be compared to one another.

The samples were concentrated during the DNA extraction, so the concentration factor needed to be matched with the concentration factor of the standard curve. The concentration factor for the standard curve was 40 and the concentrations of the other samples were matched to this. The adjusted bacterial counts of the mutant cultures and the control are shown in figure 4.2. The figure also has the overall DNA content of the samples. The scales are logarithmic since both the bacterial count and the DNA content of the wild-type sample were significantly higher than the mutants. As was expected, the bacterial count is significantly higher in all samples after 8 weeks. This suggests that some intracellular DNA probably was lost at the first time point, which was after 6 weeks, rendering lower bacterial counts. Interestingly the amount of overall DNA is lower after 8 weeks than it was after 6 weeks, suggesting that some mycobacterial DNA was lost in all samples during the two weeks between the time points. It is unlikely that this is a pipetting error since the same trend is seen in all samples. The simplest explanation is that the bacterial

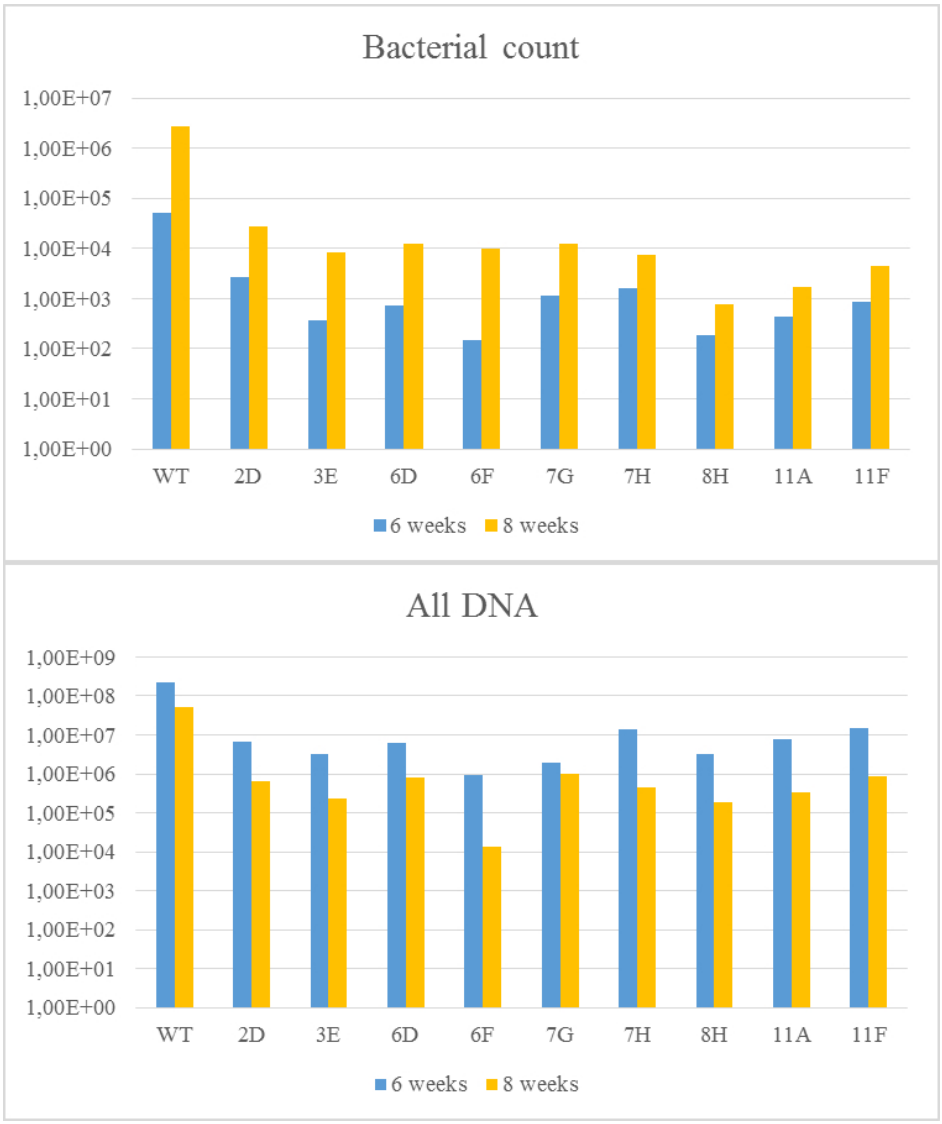

Figure 4.2: The bacterial count as CFU/μl and the overall DNA content of the samples from the third screen at both time points. WT stands for the wild-type control grown alongside the mutants.

count has declined and instead of being incorporated into the biofilm, the released DNA has been degraded.

Figure 4.3 shows the amounts of biomass and eDNA produced by the bacteria in the third screen. The results have been normalized with the samples' bacterial count allowing a better comparison of the biomass and eDNA contents. Without this normalization the strains with low bacterial count but high biomass production and high bacterial count but low biomass production would be hard to distinguish from one another. What is interesting in these results, is that the amount of biomass per bacterium is lower in all samples after 8 weeks. This suggests that there is either less biomass or more bacteria than there was after 6 weeks. The bacterial counts were significantly higher at the second time point, after 8 weeks, due to the improved protocol, so the higher biomass production

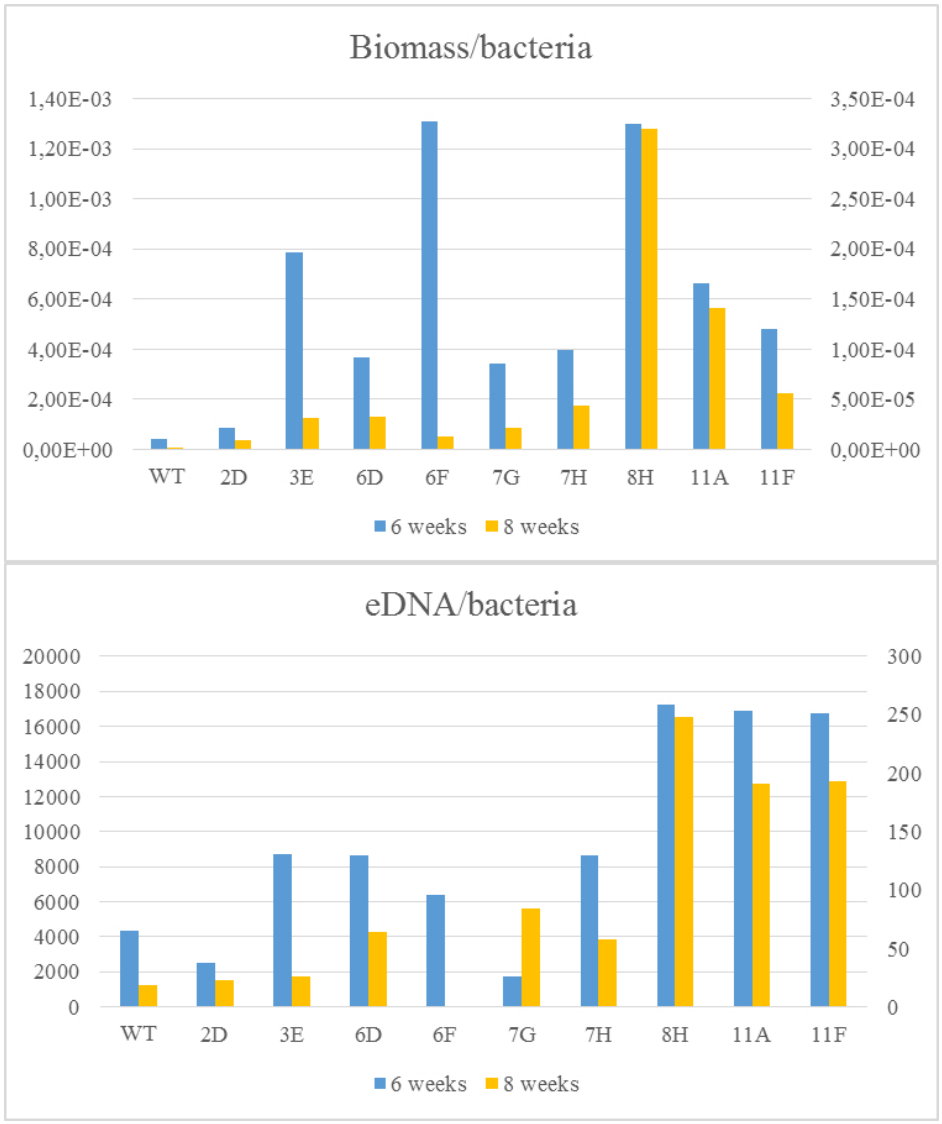

Figure 4.3: The biomass and eDNA production from the third screen at both time points. The right axis is used for the results after 8 weeks, which was the second time point. WT stands for the wild-type control grown alongside the mutants.

is probably just a result of the altered protocol.

The altered protocol also affects the results of the eDNA production. Since some of the intracellular DNA was also lost at the 6 week time point, the amount of eDNA is actually lower than the results show. According to the graph the amount of eDNA was significantly higher in all samples after 6 weeks, so this again supports the hypothesis that some of the intracellular DNA was indeed lost.

At both time points all the mutants had significantly lower bacterial counts than the wild-type and the overall DNA content was also lower in mutants than in the wild-type. However, the biomass production was higher in all mutants compared to the wild-type. The amount of eDNA was also higher in most mutants at both time points, when compared

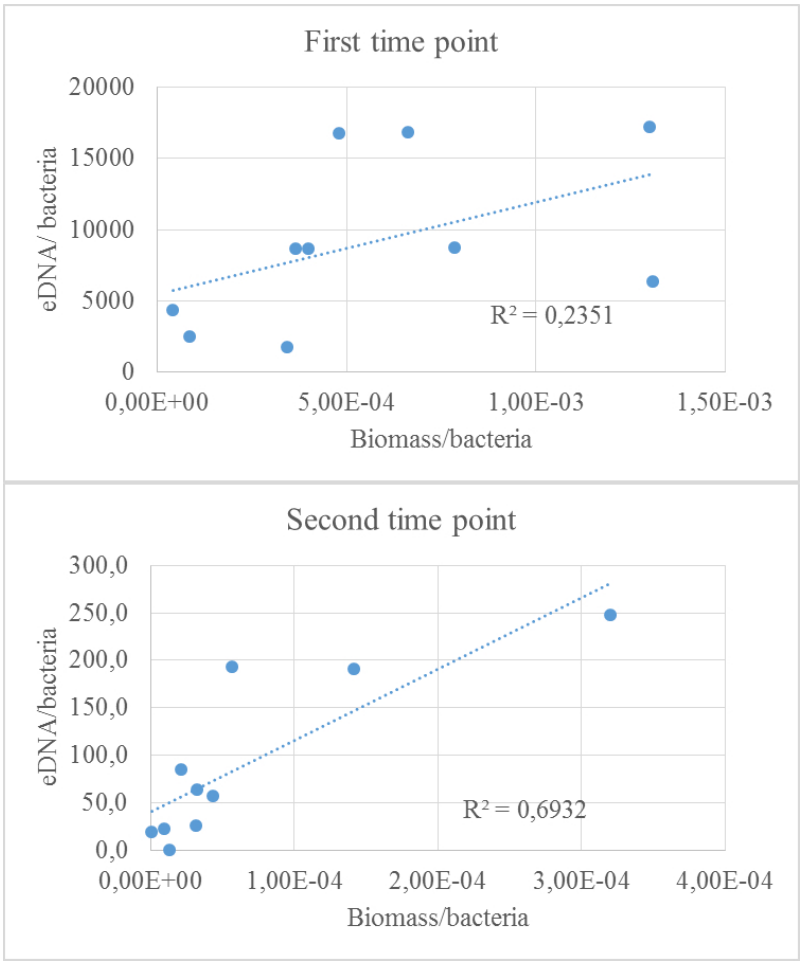

Figure 4.4: The linear correlation between eDNA and biomass production at both time points. The correlation coefficients are shown in the graphs.

to the wild-type. At both time points the mutants 8H, 11A and 11F had the highest eDNA content and this content was significantly higher than the wild-type or any other mutant. The same mutants also produced quite significant amounts of biomass and the production was a lot higher than the wild-type. Even though these highest biomass producers were also the highest eDNA producers, overall there was no correlation between biomass and eDNA production at the first time point, but some correlation at the second time point, as can be seen from figure 4.4. The lack of correlation at the first time point may be caused by the distorted results of the eDNA content. The bacterial counts shouldn't have an effect, since both eDNA and biomass content are achieved by dividing the obtained result with the bacterial count. However, looking at the lower graph in figure 4.4, the samples are quite scattered on both sides of the trendline. A third measurement would be needed before any proper conclusions can be drawn from this data.

The mutant 2D always resembled the wild-type the most. It had the highest bacterial count out of the mutants at both time points. It also had the lowest biomass and eDNA

contents. After 6 weeks, at the first time point, the culture of the mutant 2D actually had less eDNA than the wild-type culture. If the mutant 2D resembles the wild-type enough, it could be used as a kanamycin resistant control in future experiments. However, in the second screen this mutant did not form a pellicle, which is a significant difference in the appearance of the biofilm, when compared to the wild-type. On the other hand, this strain could be used to study the importance of the pellicle formation.

Another mutant with interesting results is 6F. After 8 weeks the culture contains significantly less mycobacterial DNA than any other culture. It also has practically no eDNA at the second time point, after 8 weeks, even though after 6 weeks there was more eDNA than in the wild-type sample. The amount of biomass is also completely different between the two time points. The mutant 6F had the highest amount of biomass after 6 weeks but the second lowest amount of biomass of the mutants after 8 weeks. Since two different culture tubes were analyzed at the two different time points, it is possible that these differences are results of errors that have occurred during sampling or some other point of the protocol. Due to the inconsistency of the results, the growth rate of the mutant 6F was not determined, but the mutant was stored as a glycerol stock for possible further experiments.

The mutant strains with consistent results at both time points for both biomass and eDNA production were chosen for the growth rate determination. The most interesting ones were the high biomass and eDNA producers 8H, 11A and 11F, which differed significantly from the wild-type. The 2D was also chosen in order to study its resemblance with the wild-type further. The mutant 7G had similar amount of biomass at both time points in reference to the other mutants and the wild-type, but the amounts of eDNA were not consistent. The mutants 7H and 6D were both in between the high producers and the control at both time points and their results were also considered consistent, so their growth rates were also determined.

4.5 Biofilm formation in aerobic conditions

Another interesting factor, which affected the selection of the mutants was the formation of pellicle. The 24-well plates prepared for glycerol stock preparation were also imaged to see the differences in the biofilms of the mutants compared to the wild-type. The images of the biofilms are shown in figure 4.5. The mutants forming pellicles were 3E, 6F, 8H, 11A and 11F. The yellow color is most likely the carotenoid pigment caused by exposure to the light. Since the mutants were all on the same 24-well plate, they have all had the same amount of light exposure. Interestingly, some of the mutants have a lot more of this yellow pigment than the others. It seems that in general the pellicle forming mutants also produce more carotenoid pigment.

The macrostructures of the mutant biofilms are also different. The mutants, such as 6F and 8H, contain clear cord-like structures. Some of the mutants, like 7H and 11F, have

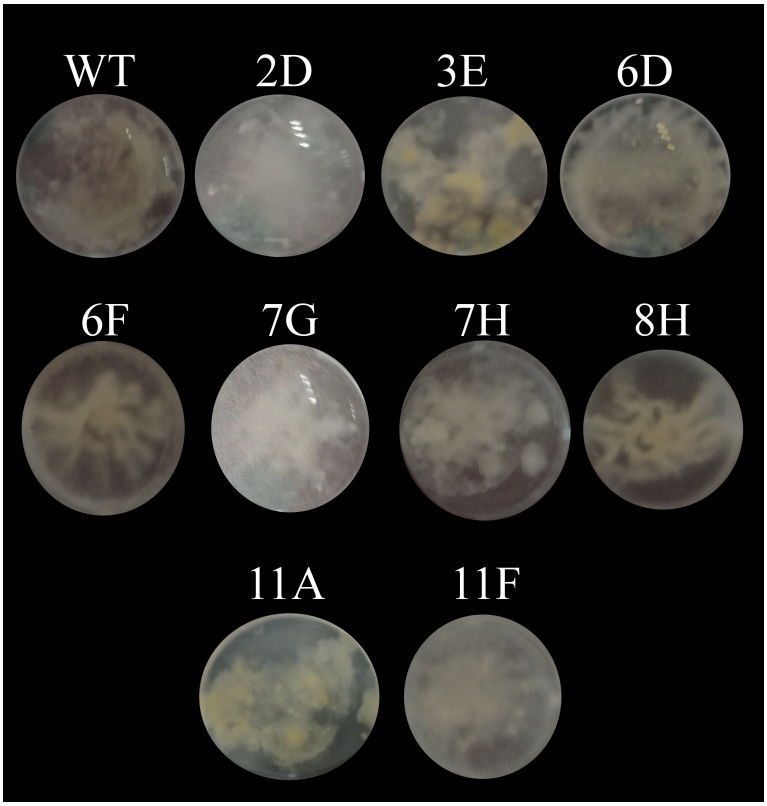

Figure 4.5: Images of the wells containing the mutants and the control. The mutants 3E, 6F, 8H, 11A and 11F had formed pellicles as well as the wild-type control, which is marked WT.

almost billowy biofilm at the bottom. In most of the mutants the biofilm also seems a bit more scattered and clumpy than in the wild-type.

The pellicle formation was also compared to the results of the third screen. The three highest biomass and eDNA producers also produced pellicles. The pellicle producing strains had higher biomass and eDNA content on average than the non-pellicle forming strains at both time points. The calculated averages are listed in table 4.2. At both time points the average of the amount of eDNA is around twice as high in pellicle forming strains. The differences between the averages of amounts of biomass are even higher. Also after 6 weeks the pellicle forming mutant strains had the highest amounts of biomass

Table 4.2: The averages of the biomass and eDNA contents calculated for pellicle and non-pellicle forming strains separately. The wild-type control is included in the results as a pellicle forming strain.

	After 6 weeks		After 8 weeks	
	Biomass	eDNA	Biomass	eDNA
No pellicle	$2.98*10^{-4}$	5 400	$2.67*10^{-5}$	57
Pellicle	$7.63*10^{-4}$	11 712	$9.40*10^{-5}$	113

per bacterium. However, the wild-type *M. marinum* had the lowest amount of biomass, even less than the non-pellicle forming strains.

At the second time point, after 8 weeks, the mutants 8H, 11A and 11F had the highest amount of biomass / bacterium, but the pellicle forming mutants 6F and 3E had significantly less biomass than they had after 6 weeks. Since the mutant 6F also had very low amounts of overall DNA, eDNA and low bacterial counts, it could be that the particular culture chosen for the analysis at the second time point had not grown properly for some reason. It is unlikely that the two week difference between the time points would have an effect, since the incubation time is so long. The mutant 3E also had relatively low amounts of eDNA, but the amount of overall DNA and the bacterial count seemed normal, when compared to the results of the other mutants.

4.6 Growth rate

The strains 2D, 6D, 7H, 8H, 11A and 11F were chosen for the growth rate determination. The wild-type was also grown as a control. Previously the growth rate and the correlation between the optical density and the bacterial count have been determined for wild-type *M. marinum* at higher Tween®80 concentrations [95]. Since the Tween®80 inhibits biofilm formation, the previously determined correlations most likely won't apply to the cultures grown at lower Tween®80 concentrations.

After three days there was a significant drop in the bacterial counts in all samples. The drop could be a result of the change of the dilution medium, since on previous days the growth medium was used for dilution and on the last two days phosphate buffered saline was used as a dilution medium. However, there should not be this dramatic effect, since the phosphate buffered saline is used in infections as a dilution medium. All the dilutions were also carried out within two hours of the first absorbance measurement. Either the phosphate buffered saline wasn't what it was supposed to be or the bacteria residing in it die a lot faster than previously believed. Due to the decline in bacterial counts the growth rates were determined based on the three first days.

The increase rates of bacterial count and optical density are shown in table 4.3. The rates have been normalized with the wild-type to make the comparison of the values easier. In all mutant cultures the optical density increases faster than in the wild-type cultures. The mutants with the slowest increase in optical density, and therefore the mutants closest to the wild-type, are mutants 2D and 6D. The strain with the fastest increase in optical density is mutant 7H with over 20 % faster increase in optical density than the wild-type. The mutant 2D has only 6 % faster increase in optical density.

The generation times of the mutants vary a lot more than the increase rates of optical density. The mutants 2D and 11F had faster generation times than the wild-type. The generation times of the other mutants, however, are significantly slower than the wild-type. The mutant 6D has the slowest generation time, only 30 % of the wild-type generation

Table 4.3: The growth rates of the mutants measured as change in bacterial counts and absorbance in reference to wild-type *M. marinum*. WT stands for wild-type control, OD for optical density and BC for bacterial count.

Strain	OD	BC	OD/BC
WT	1.00	1.00	1.00
2D	1.06	1.12	0.95
6D	1.08	0.30	3.64
7H	1.23	0.60	2.07
8H	1.18	0.39	3.04
11A	1.12	0.60	1.85
11F	1.18	1.30	0.91

time. The mutant 8H is not a lot faster, only 39 % of the wild-type generation time.

What really is interesting biofilm-vice, is the relation between the generation time and the increase rate of optical density. The increase in optical density is caused by both increase in the bacterial count as well as increase in the amount of biofilm. Since the rates have been normalized with the wild-type rates, the increase rates closest to 1 are closest to normal and the increase rates farthest from it are the most abnormal. The strains 2D and 11F stand out as the strains closest to the wild-type. Both of them have a bit higher increase rates of both optical density and bacterial count as compared to the wild-type. Also for both strains the increase rate of optical density is slightly slower than the increase rate of bacterial count. It seems that they produce somewhat similar amounts of biofilm per bacterium as the wild-type. The faster generation time may make them seem like more efficient biofilm producers, since the optical density increases faster. However, the increase in bacterial count accounts for the faster increase in optical density.

The rest of the strains seem like more efficient biofilm producers than the wild-type, since their optical density increases significantly faster than the bacterial count. This is consistent with the results of the third screen. The two strains with the fastest increasing optical density, when compared to the bacterial count, are mutants 6D and 8H. In both cases the bacterial counts are rising extremely slowly, which mainly accounts for the difference when compared to the wild-type.

The correlation between the bacterial count and the optical density was also studied. The correlation coefficients and the plotted graphs are shown in figure 4.6. There is little to no correlation between the optical density and the bacterial count in strains 6D, 8H and 11A. The highest correlation coefficients are found in mutants 2D, 7H and 11F as well as the wild-type. It seems that for some of the strains an equation describing the relation between the optical density and the bacterial count could be determined with a few more replicates for each time point.

The bacteria was also grown as bottle cultures to compare the effect of the culture

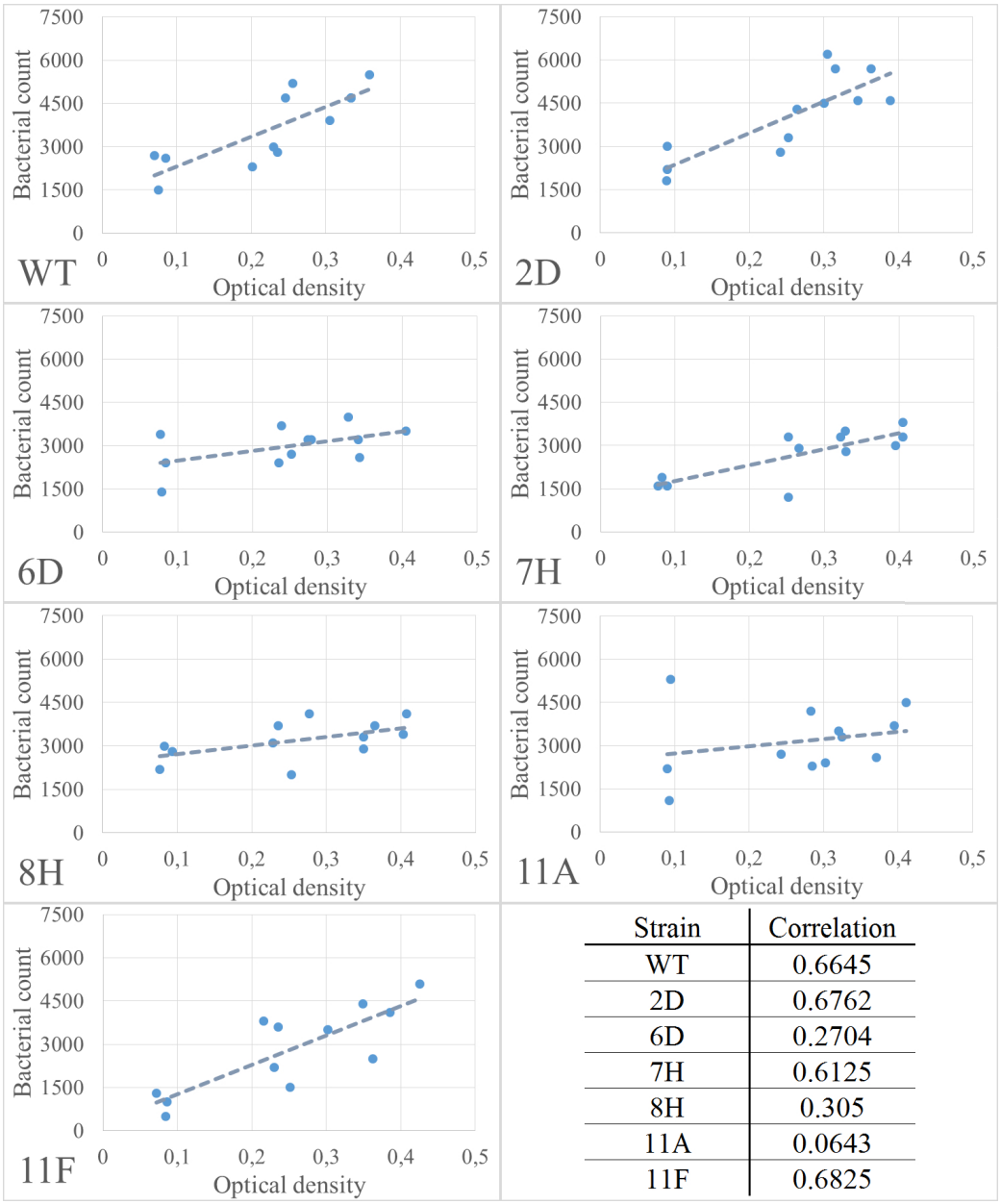

Strain	Correlation
WT	0.6645
2D	0.6762
6D	0.2704
7H	0.6125
8H	0.305
11A	0.0643
11F	0.6825

Figure 4.6: The correlations between bacterial count and optical density within the first three days. WT stands for wild-type control. The correlation coefficients are listed in the bottom right corner.

vial and the daily measurements of optical density, which required proper mixing of the culture. The bottles were grown undisturbed for four days at the same conditions as the culture tubes previously described. It is probable that the daily mixing affected the biofilm formation somehow. The results of the comparison are shown in table 4.4.

There are only small differences in the optical densities between bottle and tube cultures. In general the optical densities are a little higher in the bottle cultures. This could possibly be a result of biofilm breakage caused by the daily mixing in the tube cultures. The bacterial counts are also lower in the tube cultures than in bottles, except for the

Table 4.4: The optical densities and the bacterial counts measured from the bottle and tube cultures on the fourth day. The values of optical density and bacterial count from the culture tubes are averages of the three tubes. WT stands for wild-type control. OD stands for optical density and BC for bacterial count.

Strain	OD in a bottle	OD in a tube	BC in a bottle	BC in a tube	OD/BC in a bottle	OD/BC in a tube
WT	0.42	0.43	1 550	1 800	0.00027	0.00030
2D	0.52	0.44	1 750	530	0.00030	0.00095
6D	0.53	0.46	1 350	130	0.00039	0.00382
7H	0.49	0.45	1 400	200	0.00035	0.00281
8H	0.50	0.45	1 000	500	0.00050	0.00104
11A	0.51	0.45	1 600	200	0.00032	0.00311
11F	0.42	0.45	950	870	0.00044	0.00053

wild-type. However, the differences of bacterial counts between bottles and tubes are much greater than the differences in optical densities. The drop in bacterial counts, which was observed in the culture tubes, possibly also occurred in the culture bottles. The bacterial counts are so much higher in the culture bottles that if a drop in bacterial counts occurred, ether it was significantly smaller in culture bottles or the peak of the bacterial counts was a lot higher in them.

The bacterial counts in the wild-type tube cultures are a bit higher than in the culture bottle. It seems that the wild-type *M. marinum* grew slightly better in the culture tube. The ratio between the optical density and bacterial count is very similar in both cultures, suggesting similar biofilm formation. The mutant strain 11F also had similar results on the fourth day in both tube and bottle cultures. Interestingly this mutant grew poorest out of all strains in the culture bottles, but was second best growing in the tube cultures. It seems that the daily vigorous mixing affected the wild-type and the mutant 11F less than others if at all. One explanation could be that they have stronger cell wall structure, which then tolerates the mixing better. According to the literature the cell wall structure has a great impact on the structure of the biofilm.

The rest of the mutant strains had significantly lower bacterial counts in the tube cultures than in the bottles, even though the optical densities were similar in both. In many of these strains there are actually ten-fold differences between ratios of optical density and bacterial count. With the strain 2D the ratio in the culture bottle is one third of the ratio in tube cultures. With the strain 8H the ratio in the bottle culture is half of the ratio in the tube cultures. It could be that these poorly grown strains went into the biofilm producing mode. The formed biofilm was constantly dispersed, so the bacteria kept producing more of the biofilm matrix and therefore they weren't dividing. With this hypothesis the strains, which were mostly affected by the mixing, have the weakest biofilms. These strains are the mutants 6D, 7H and 11A. Then the wild-type biofilm and the biofilm of the mutant

11F would be the strongest ones. However, the experiment should be repeated to verify the results, since there was only one bottle culture of each of the strains.

5. CONCLUSIONS

Tuberculosis has infected the mankind for at least 4 000 years. The course of the *M. tuberculosis* infection depends on the host's immune system, the initial bacterial load and the bacterial strain. The bacteria is phagocytosed by macrophages and dendritic cells. Then the bacteria residing in the phagosome inhibit the phagosome maturation and the macrophage becomes infected. The infected cells aggregate and attract uninfected cells to the aggregates forming a granuloma. These granulomas are a characteristic sign of the *M. tuberculosis* infection. The granulomas protect the bacteria from the host's immune system, but they also restrict the growth of the bacteria. The bacteria residing in the granuloma may enter dormancy, establishing a latent infection. If the infection remains active, the bacteria escape from the granuloma and help to form new granulomas. The *M. tuberculosis* growth in lungs causes extensive damage, eventually leading to suffocation. The main problem with tuberculosis infections is, that they are often resistant to several antibiotics and require long periods of treatment with several different antibiotics.

The infection mechanisms of *M. marinum* are very similar to *M. tuberculosis* and they share many virulence factors. They have different natural hosts and the generation time of *M. marinum* significantly shorter. *M. marinum* infection in zebrafish has therefore been used to study these infection mechanisms in a safer and faster way. *M. marinum* is also easier to culture since it survives in liquid media. The zebrafish are also an inexpensive model, which requires relatively small facilities.

The persistent biofilms are believed to be the basis of the antibiotic resistance of mycobacteria, like *M. tuberculosis* and *M. marinum*. The mycobacterial biofilms can crudely be divided to two groups based on the location of their adherence. Pellicles are formed at the air-liquid interphase and they are attached to the sides of the culture and pellets are formed at the bottom and they are attached to the bottom of the container. The formation of the biofilm depends on the growth conditions and for many mycobacterial species nutrient depleted media seems to induce biofilm formation. However, in this experiment it seemed that *M. marinum* biofilms were formed significantly faster in richer media. It could be that the biofilm formation was in fact more efficient in the depleted media, but the bacterial growth and cell division was completely stalled and therefore the cultures died before proper biofilm could be produced, so only the strongest mutant strains survived and produced visible biofilms. This could explain the poor bacterial growth in the first and the second screen. During the experiment the number of strains reduced from 3 500

to 9 and finally to 6 for the growth rate measurements. In the first and second screens, the reduction of the strains was mainly a result of the non-growing cultures instead of a normal appearance of the biofilms. Therefore it is hard to approximate the mount of biofilm related genes from these results. However, it seems that all the strains chosen for the third screen had somewhat abnormal biofilms when compared to the wild-type. It seems that there are more genes related to the biofilm formation than was approximated in the beginning of this experiment, since at least 5 strains with clearly abnormal biofilm formation were found.

The ECM of the *M. marinum* biofilm contains several different lipids, proteins and eDNA. In this experiment only the amount of eDNA was studied separately. In the third screen the amount of DNA was determined before and after DNase I treatment. There were three mutants, 8H, 11A and 11F, that had significantly more eDNA in the cultures than any of the others or the wild-type. All of these three mutants also formed pellicles. The other two pellicle-forming mutants, 3E and 6F, did not stand out as eDNA producers. In fact there was practically no eDNA found in the mutant 6F culture at the second time point, but the amount of overall DNA was also low as well as the amount of biomass. It seems likely that for some reason the particular culture had grown poorly. The results of the 6F at the second time point should therefore be considered unreliable.

At the first time point in the third screen the pellicle-forming mutants clearly had the highest amounts of biomass per bacterium. However, at the second time point the amount of biomass was smaller in mutants 3E and 6F. It could be that there were some problems also in the 3E culture as well as in the culture of 6F. Another possibility is that the mutations in these two strains are somewhat less stable, resulting in more variable phenotypes. Since the protocol was improved for the second time point, the results of that time point should be more reliable than the results of the first time point. However, only one tube was measured per strain at both time points, which lowers the reliability of the results greatly. This is why all the mutants with dissimilar results at the two time points were left out from the growth rate analysis.

The results of the third screen suggest that there might be a correlation between pellicle formation and higher biomass formation. If this is the case, then the pellicle most likely contains more biomass per bacterium than the bottom biofilm. On the other hand, the wild-type *M. marinum*, which also forms the pellicle, had the lowest amounts of biomass per bacterium in the cultures. In fact, all the mutants produced more biomass per bacterium than the wild-type in both the third screen as well as in the growth rate determinations. The eDNA isn't stained by crystal violet, so high eDNA content in the biofilm doesn't explain high biomass content and there was no correlation between them either, even though the three highest biomass producers were also the highest eDNA producers.

The current hypothesis is that mycobacteria are either actively dividing or producing biofilm [55], and the results of this screen seem to support that hypothesis, since the high

biomass producers had low bacterial counts and vice versa. The high biomass therefore reflects higher amounts of biofilm matrix, if the bacterial counts are low. It seems that there might be reverse correlation between the bacterial counts and the biomass content. The linear correlation between these two, however, is very low. Another option is that the high eDNA producers, which also have low bacterial counts are dying faster than the other strains and the DNA released from the dead cells is incorporated to the biofilm.

The amount of biomass also seems to correlate with the optical density to some extent. The correlation between bacterial count and optical density was actually surprisingly high even at this low concentrations of Tween®80. Enough high correlation allows the bacterial count to be approximated from the optical density. The equation describing the relation between optical density and bacterial count should be determined to all mutants with high enough correlation and the wild-type. These equations could later be used in infection experiments on zebrafish.

In the third screen mutant 2D resembled the wild-type most, but in the growth rate determinations mutant 11F had the closest resemblance with the wild-type. The growth rate was determined in a richer medium, so it could be that the nutrient deprived growth medium affected mutant 11F more than others. Also the 2D strain does not produce pellicle, but the strain 11F does. Therefore the mutant 11F might actually work as a better kanamycin resistant control in future experiments. Mutant 11F was also almost as resistant to mixing as the wild-type, which was the most resistant out of the tested strains. This suggests that these two strains have the strongest cell walls, which might also lead to stronger biofilms. However, the mutation of 11F is not known, so wild-type control should be used alongside it. The strain 2D could be used to study the effects of pellicle formation and see how the lack of pellicle *in vitro* affects the infection outcome in zebrafish.

If the experiment should be repeated, it would be better to use a richer growth medium also in the screens, so the effect of the nutrient deprived growth medium could be ruled out. The mutants grown in richer media were also more likely to grow on agar, so there would be more reliable and efficient means for bacterial count determination. The qPCR only measures bacterial content, and if the relation between the eDNA and the bacteral varies between strains, which is likely in mutant strains, the qPCR becomes very unreliable. On the other hand, the qPCR could be used for more reliable eDNA measurement if the standard was also measured before and after the DNase treatment. Also the colonies picked from the plates should not be so small. The smaller colonies most likely increase the risk of growth defects. The results of the experiments are also more worthwhile, if the strains do not grow unusually slow.

It is likely that only some of these mutant strains harbor a knockout mutation. The MycoMar T7 phage contains T7 promoters flanking the transposon. The T7 promoter is highly active, so the adjacent segments of genome are overexpressed. It could be that

these high biomass or eDNA producers are actually overexpressing the genes close to the transposon and this overexpression causes the excess biofilm formation. The mutant 2D is more likely to have a knockout mutation, since it does not form the pellicle. Also it is not known, whether these strains contain only one or several mutations. It is not only possible, but also likely, that some of these strains actually contain more than one integrated transposon. Therefore these mutants should be sequenced to determine, what kind of mutations they have.

The effect of the mutation could be studied further with antibiotics and other biocides to see if the altered biofilm also alters the resistance to these biocides *in vitro*. Since the biofilm is believed to act as a protection against biocides, the strains producing higher amounts of biomass and therefore also more biofilm matrix, should have higher tolerance against biocides. The sequencing could also bring more insight to biofilm formation, possibly revealing new genes and metabolic pathways related to it.

These mutant strains could also be studied *in vivo* in the zebrafish model. The zebrafish could be infected with a mutant strain and the infection outcome could be compared to the wild-type *M. marinum*. The bacterial loads of the infection could be studied at different time points post infection. Also the effect of different antibiotics against the infection could be studied as well as the structure of granulomas. It would be really interesting to study the correlation between biofilms and granulomas. Does the abnormal biofilm formation affect the structure and formation of granulomas?

The most interesting results are achieved if the affected genes have orthologues in the *M. tuberculosis* genome. If the overexpression of a certain gene results in higher biofilm formation, could the knockout strain lacking the same particular gene have deficient biofilm formation? The orthologues in the *M. tuberculosis* genome will also provide important insight into the metabolic pathways associated with biofilm formation in *M. tuberculosis* and the infection outcomes of these *M. marinum* mutants in zebrafish may give more information about the infection mechanisms of *M. tuberculosis*. The data gathered from the future experiments of these mutant strains could possibly lead to design of new and more efficient drugs against mycobacterial infections, including tuberculosis.

REFERENCES

[1] "World Health Organization: Tuberculosis (TB)." `http://www.who.int/mediacentre/factsheets/fs104/en/`, 2017. Accessed October 13th 2017.

[2] K. J. Seung, S. Keshavjee, and M. L. Rich, "Multidrug-resistant tuberculosis and extensively drug-resistant tuberculosis," *Cold Spring Harbor perspectives in medicine*, 2015.

[3] A. K. Ojha, A. D. Baughn, D. Sambandan, T. Hsu, X. Trivelli, Y. Guerardel, A. Alahari, L. Kremer, W. R. Jacobs, and G. F. Hatfull, "Growth of *Mycobacterium tuberculosis* biofilms containing free mycolic acids and harbouring drug-tolerant bacteria," *Molecular microbiology*, vol. 69, no. 1, pp. 164–174, 2008.

[4] J. van Ingen, Z. Rahim, A. Mulder, M. J. Boeree, R. Simeone, R. Brosch, and D. van Soolingen, "Characterization of *Mycobacterium orygis* as *M. tuberculosis* complex subspecies," *Emerging infectious diseases*, vol. 18, no. 4, p. 653, 2012.

[5] A. Ojha, M. Anand, A. Bhatt, L. Kremer, W. R. Jacobs, and G. F. Hatfull, "GroEL1: a dedicated chaperone involved in mycolic acid biosynthesis during biofilm formation in mycobacteria," *Cell*, vol. 123, no. 5, pp. 861–873, 2005.

[6] J. P. Richards and A. K. Ojha, "Mycobacterial biofilms," in *Molecular Genetics of Mycobacteria, Second Edition*, pp. 773–784, American Society of Microbiology, 2014.

[7] E. Bardouniotis, H. Ceri, and M. E. Olson, "Biofilm formation and biocide susceptibility testing of *Mycobacterium fortuitum* and *Mycobacterium marinum*," *Current microbiology*, vol. 46, no. 1, pp. 0028–0032, 2003.

[8] I. Smith, "*Mycobacterium tuberculosis* pathogenesis and molecular determinants of virulence," *Clinical microbiology reviews*, vol. 16, no. 3, pp. 463–496, 2003.

[9] E. Cambau and M. Drancourt, "Steps towards the discovery of *Mycobacterium tuberculosis* by Robert Koch, 1882," *Clinical Microbiology and Infection*, vol. 20, no. 3, pp. 196–201, 2014.

[10] J. Lumio, "Tuberkuloosi," *Lääkärikirja Duodecim*, 2016.

[11] D. Heemskerk, M. Caws, B. Marais, and J. Farrar, *Tuberculosis in Adults and Children*. Springer, 2016.

[12] S. Ahmad, "Pathogenesis, immunology, and diagnosis of latent *Mycobacterium tuberculosis* infection," *Clinical and Developmental Immunology*, vol. 2011, 2010.

[13] D. M. Tobin and L. Ramakrishnan, "Comparative pathogenesis of *Mycobacterium marinum* and *Mycobacterium tuberculosis*," *Cellular microbiology*, vol. 10, no. 5, pp. 1027–1039, 2008.

[14] Z. A. Malik, G. M. Denning, and D. J. Kusner, "Inhibition of Ca^{2+} signaling by *Mycobacterium tuberculosis* associated with reduced phagosome-lysosome fusion and increased survival within human macrophages," *Journal of Experimental Medicine*, vol. 191, no. 2, pp. 287–302, 2000.

[15] L. E. Via, D. Deretic, R. J. Ulmer, N. S. Hibler, L. A. Huber, and V. Deretic, "Arrest of mycobacterial phagosome maturation is caused by a block in vesicle fusion between stages controlled by rab5 and rab7," *Journal of Biological Chemistry*, vol. 272, no. 20, pp. 13326–13331, 1997.

[16] E. H. Noss, R. K. Pai, T. J. Sellati, J. D. Radolf, J. Belisle, D. T. Golenbock, W. H. Boom, and C. V. Harding, "Toll-like receptor 2-dependent inhibition of macrophage class II MHC expression and antigen processing by 19-kDa lipoprotein of *Mycobacterium tuberculosis*," *The Journal of Immunology*, vol. 167, no. 2, pp. 910–918, 2001.

[17] H. E. Volkman, H. Clay, D. Beery, J. C. Chang, D. R. Sherman, and L. Ramakrishnan, "Tuberculous granuloma formation is enhanced by a mycobacterium virulence determinant," *PLoS biology*, vol. 2, no. 11, p. e367, 2004.

[18] C. L. Cosma, O. Humbert, and L. Ramakrishnan, "Superinfecting mycobacteria home to established tuberculous granulomas," *Nature immunology*, vol. 5, no. 8, p. 828, 2004.

[19] M. P. Etna, E. Giacomini, M. Pardini, M. Severa, D. Bottai, M. Cruciani, F. Rizzo, R. Calogero, R. Brosch, and E. M. Coccia, "Impact of *Mycobacterium tuberculosis* RD1-locus on human primary dendritic cell immune functions," *Scientific reports*, vol. 5, 2015.

[20] B. McLaughlin, J. S. Chon, J. A. MacGurn, F. Carlsson, T. L. Cheng, J. S. Cox, and E. J. Brown, "A mycobacterium ESX-1-secreted virulence factor with unique requirements for export," *PLOS pathogens*, vol. 3, no. 8, p. e105, 2007.

[21] H. E. Volkman, T. C. Pozos, J. Zheng, J. M. Davis, J. F. Rawls, and L. Ramakrishnan, "Tuberculous granuloma induction via interaction of a bacterial secreted protein with host epithelium," *Science*, vol. 327, no. 5964, pp. 466–469, 2010.

[22] J. Xu, O. Laine, M. Masciocchi, J. Manoranjan, J. Smith, S. J. Du, N. Edwards, X. Zhu, C. Fenselau, and L.-Y. Gao, "A unique mycobacterium ESX-1 protein co-secretes with CFP-10/ESAT-6 and is necessary for inhibiting phagosome maturation," *Molecular microbiology*, vol. 66, no. 3, pp. 787–800, 2007.

[23] E. M. Weerdenburg, A. M. Abdallah, S. Mitra, K. De Punder, N. N. Van Der Wel, S. Bird, B. J. Appelmelk, W. Bitter, and A. M. Van Der Sar, "ESX-5-deficient *Mycobacterium marinum* is hypervirulent in adult zebrafish," *Cellular microbiology*, vol. 14, no. 5, pp. 728–739, 2012.

[24] L. I. Klepp, M. Soria, F. C. Blanco, M. V. Bianco, M. P. Santangelo, A. A. Cataldi, F. Bigi, *et al.*, "Identification of two proteins that interact with the Erp virulence factor from *Mycobacterium tuberculosis* by using the bacterial two-hybrid system," *BMC Molecular Biology*, vol. 10, no. 3, pp. 615–624, 2009.

[25] K. Pethe, S. Alonso, F. Biet, G. Delogu, *et al.*, "The heparin-binding haemagglutinin of *M. tuberculosis* is required for extrapulmonary dissemination," *Nature*, vol. 412, no. 6843, p. 190, 2001.

[26] J. L. Flynn, "Lessons from experimental *Mycobacterium tuberculosis* infections," *Microbes and Infection*, vol. 8, no. 4, pp. 1179–1188, 2006.

[27] F. M. Collins, V. Montalbine, and N. E. Morrison, "Growth and immunogenicity of photochromogenic strains of mycobacteria in the footpads of normal mice.," *Infection and immunity*, vol. 11, no. 5, pp. 1079–1087, 1975.

[28] M. Parikka, M. M. Hammarén, S.-K. E. Harjula, N. J. Halfpenny, K. E. Oksanen, M. J. Lahtinen, E. T. Pajula, A. Iivanainen, M. Pesu, and M. Rämet, "*Mycobacterium marinum* causes a latent infection that can be reactivated by gamma irradiation in adult zebrafish," *PLoS pathogens*, vol. 8, no. 9, p. e1002944, 2012.

[29] A. H. Meijer, "Protection and pathology in TB: learning from the zebrafish model," in *Seminars in immunopathology*, vol. 38, pp. 261–273, Springer, 2016.

[30] D. Traver, P. Herbomel, E. E. Patton, R. D. Murphey, J. A. Yoder, G. W. Litman, A. Catic, C. T. Amemiya, L. I. Zon, and N. S. Trede, "The zebrafish as a model organism to study development of the immune system," *Advances in immunology*, vol. 81, pp. 254–330, 2003.

[31] J. A. Yoder, "Investigating the morphology, function and genetics of cytotoxic cells in bony fish," *Comparative Biochemistry and Physiology Part C: Toxicology & Pharmacology*, vol. 138, no. 3, pp. 271–280, 2004.

[32] H. Clay, J. M. Davis, D. Beery, A. Huttenlocher, S. E. Lyons, and L. Ramakrishnan, "Dichotomous role of the macrophage in early *Mycobacterium marinum* infection of the zebrafish," *Cell host & microbe*, vol. 2, no. 1, pp. 29–39, 2007.

[33] L. E. Swaim, L. E. Connolly, H. E. Volkman, O. Humbert, D. E. Born, and L. Ramakrishnan, "*Mycobacterium marinum* infection of adult zebrafish causes caseating granulomatous tuberculosis and is moderated by adaptive immunity," *Infection and immunity*, vol. 74, no. 11, pp. 6108–6117, 2006.

[34] R. van Crevel, T. H. Ottenhoff, and J. W. van der Meer, "Innate immunity to *Mycobacterium tuberculosis*," *Clinical microbiology reviews*, vol. 15, no. 2, pp. 294–309, 2002.

[35] A. M. Van Der Sar, A. M. Abdallah, M. Sparrius, E. Reinders, C. M. J. E. Vandenbroucke-Grauls, and W. Bitter, "*Mycobacterium marinum* strains can be divided into two distinct types based on genetic diversity and virulence," *Infection and immunity*, vol. 72, no. 11, pp. 6306–6312, 2004.

[36] L. M. Stamm and E. J. Brown, "*Mycobacterium marinum*: the generalization and specialization of a pathogenic mycobacterium," *Microbes and infection*, vol. 6, no. 15, pp. 1418–1428, 2004.

[37] J. Karlsson, J. von Hofsten, and P.-E. Olsson, "Generating transparent zebrafish: a refined method to improve detection of gene expression during embryonic development," *Marine Biotechnology*, vol. 3, no. 6, pp. 522–527, 2001.

[38] V. Torraca, C. Cui, R. Boland, J.-P. Bebelman, A. M. van der Sar, M. J. Smit, M. Siderius, H. P. Spaink, and A. H. Meijer, "The CXCR3-CXCL11 signaling axis mediates macrophage recruitment and dissemination of mycobacterial infection," *Disease models & mechanisms*, vol. 8, no. 3, pp. 253–269, 2015.

[39] S. Akram and S. Bhimji, "*Mycobacterium marinum*," 2017.

[40] J. M. Davis, H. Clay, J. L. Lewis, N. Ghori, P. Herbomel, and L. Ramakrishnan, "Real-time visualization of mycobacterium-macrophage interactions leading to initiation of granuloma formation in zebrafish embryos," *Immunity*, vol. 17, no. 6, pp. 693–702, 2002.

[41] C. Cambier, K. K. Takaki, R. P. Larson, R. E. Hernandez, D. M. Tobin, K. B. Urdahl, C. L. Cosma, and L. Ramakrishnan, "Mycobacteria manipulate macrophage recruitment through coordinated use of membrane lipids," *Nature*, vol. 505, no. 7482, p. 218, 2014.

[42] N. V. Serbina and E. G. Pamer, "Monocyte emigration from bone marrow during bacterial infection requires signals mediated by chemokine receptor CCR2," *Nature immunology*, vol. 7, no. 3, p. 311, 2006.

[43] E. Sierra-Filardi, C. Nieto, Á. Domínguez-Soto, R. Barroso, P. Sánchez-Mateos, A. Puig-Kroger, M. López-Bravo, J. Joven, C. Ardavín, J. L. Rodríguez-Fernández, *et al.*, "CCL2 shapes macrophage polarization by GM-CSF and M-CSF: identification of CCL2/CCR2-dependent gene expression profile," *The Journal of Immunology*, vol. 192, no. 8, pp. 3858–3867, 2014.

[44] W. Feng, P. Flores-Villanueva, I. Mokrousov, X. Wu, J. Xiao, W. Jiao, L. Sun, Q. Miao, C. Shen, D. Shen, *et al.*, "CCL2 -2518 (A/G) polymorphisms and tuberculosis susceptibility: a meta-analysis," *The International Journal of Tuberculosis and Lung Disease*, vol. 16, no. 2, pp. 150–156, 2012.

[45] C. L. Cosma, K. Klein, R. Kim, D. Beery, and L. Ramakrishnan, "*Mycobacterium marinum* Erp is a virulence determinant required for cell wall integrity and intracellular survival," *Infection and immunity*, vol. 74, no. 6, pp. 3125–3133, 2006.

[46] M. M. Mathews, "Studies on the localization, function, and formation of the carotenoid pigments of a strain of *Mycobacterium marinum*," *Photochemistry and Photobiology*, vol. 2, no. 1, pp. 1–8, 1963.

[47] L.-Y. Gao, R. Groger, J. S. Cox, S. M. Beverley, E. H. Lawson, and E. J. Brown, "Transposon mutagenesis of *Mycobacterium marinum* identifies a locus linking pigmentation and intracellular survival," *Infection and immunity*, vol. 71, no. 2, pp. 922–929, 2003.

[48] T. P. Stinear, T. Seemann, P. F. Harrison, G. A. Jenkin, J. K. Davies, P. D. Johnson, Z. Abdellah, C. Arrowsmith, T. Chillingworth, C. Churcher, *et al.*, "Insights from the complete genome sequence of *Mycobacterium marinum* on the evolution of *Mycobacterium tuberculosis*," *Genome research*, vol. 18, no. 5, pp. 729–741, 2008.

[49] J. L. Flynn and J. Chan, "Immunology of tuberculosis," *Annual review of immunology*, vol. 19, no. 1, pp. 93–129, 2001.

[50] D. G. Russell, "*Mycobacterium tuberculosis* and the intimate discourse of a chronic infection," *Immunological reviews*, vol. 240, no. 1, pp. 252–268, 2011.

[51] D. G. Russell, H. C. Mwandumba, and E. E. Rhoades, "*Mycobacterium* and the coat of many lipids," *The Journal of Cell Biology*, vol. 158, no. 3, pp. 421–426, 2002.

[52] L. M. Stamm, J. H. Morisaki, L.-Y. Gao, R. L. Jeng, K. L. McDonald, R. Roth, S. Takeshita, J. Heuser, M. D. Welch, and E. J. Brown, "*Mycobacterium marinum*

escapes from phagosomes and is propelled by actin-based motility," *Journal of Experimental Medicine*, vol. 198, no. 9, pp. 1361–1368, 2003.

[53] L. Hall-Stoodley and P. Stoodley, "Biofilm formation and dispersal and the transmission of human pathogens," *Trends in microbiology*, vol. 13, no. 1, pp. 7–10, 2005.

[54] M. M. Zambrano and R. Kolter, "Mycobacterial biofilms: a greasy way to hold it together," *Cell*, vol. 123, no. 5, pp. 762–764, 2005.

[55] A. Trivedi, P. S. Mavi, D. Bhatt, and A. Kumar, "Thiol reductive stress induces cellulose-anchored biofilm formation in *Mycobacterium tuberculosis*," *Nature communications*, vol. 7, p. 11392, 2016.

[56] D. De Beer, P. Stoodley, F. Roe, and Z. Lewandowski, "Effects of biofilm structures on oxygen distribution and mass transport," *Biotechnology and bioengineering*, vol. 43, no. 11, pp. 1131–1138, 1994.

[57] R. Kolter and R. Losick, "One for all and all for one," *Science*, vol. 280, no. 5361, pp. 226–227, 1998.

[58] M. R. Parsek and E. Greenberg, "Sociomicrobiology: the connections between quorum sensing and biofilms," *Trends in microbiology*, vol. 13, no. 1, pp. 27–33, 2005.

[59] G. Carter, M. Wu, D. C. Drummond, and L. E. Bermudez, "Characterization of biofilm formation by clinical isolates of *Mycobacterium avium*," *Journal of medical microbiology*, vol. 52, no. 9, pp. 747–752, 2003.

[60] J. Recht and R. Kolter, "Glycopeptidolipid acetylation affects sliding motility and biofilm formation in *Mycobacterium smegmatis*," *Journal of bacteriology*, vol. 183, no. 19, pp. 5718–5724, 2001.

[61] M. McNabe, R. Tennant, L. Danelishvili, L. Young, and L. E. Bermudez, "*Mycobacterium avium* ssp. *hominissuis* biofilm is composed of distinct phenotypes and influenced by the presence of antimicrobials," *Clinical Microbiology and Infection*, vol. 17, no. 5, pp. 697–703, 2011.

[62] L. Marsollier, P. Brodin, M. Jackson, J. Korduláková, P. Tafelmeyer, E. Carbonnelle, J. Aubry, G. Milon, P. Legras, J.-P. Saint André, *et al.*, "Impact of *Mycobacterium ulcerans* biofilm on transmissibility to ecological niches and Buruli ulcer pathogenesis," *PLoS pathogens*, vol. 3, no. 5, p. e62, 2007.

[63] S. J. Rose, L. M. Babrak, and L. E. Bermudez, "*Mycobacterium avium* possesses extracellular DNA that contributes to biofilm formation, structural integrity, and tolerance to antibiotics," *PloS one*, vol. 10, no. 5, p. e0128772, 2015.

[64] E. Julián, M. Roldán, A. Sánchez-Chardi, O. Astola, G. Agustí, and M. Luquin, "Microscopic cords, a virulence-related characteristic of *Mycobacterium tuberculosis*, are also present in nonpathogenic mycobacteria," *Journal of bacteriology*, vol. 192, no. 7, pp. 1751–1760, 2010.

[65] A. Sánchez-Chardi, C. Brambilla, E. Julián, and M. Luquin, "Cording, a virulence-related characteristic of mycobacteria, analysis using SEM," *Microscopy and Microanalysis*, vol. 18, no. S5, pp. 21–22, 2012.

[66] L.-Y. Gao, F. Laval, E. H. Lawson, R. K. Groger, A. Woodruff, J. H. Morisaki, J. S. Cox, M. Daffe, and E. J. Brown, "Requirement for *kasB* in *Mycobacterium* mycolic acid biosynthesis, cell wall impermeability and intracellular survival: implications for therapy," *Molecular microbiology*, vol. 49, no. 6, pp. 1547–1563, 2003.

[67] T. Fukuda, T. Matsumura, M. Ato, M. Hamasaki, Y. Nishiuchi, Y. Murakami, Y. Maeda, T. Yoshimori, S. Matsumoto, K. Kobayashi, *et al.*, "Critical roles for lipomannan and lipoarabinomannan in cell wall integrity of mycobacteria and pathogenesis of tuberculosis," *MBio*, vol. 4, no. 1, pp. e00472–12, 2013.

[68] H. Ren, L. G. Dover, S. T. Islam, D. C. Alexander, J. M. Chen, G. S. Besra, and J. Liu, "Identification of the lipooligosaccharide biosynthetic gene cluster from *Mycobacterium marinum*," *Molecular microbiology*, vol. 63, no. 5, pp. 1345–1359, 2007.

[69] A. Ortalo-Magne, A. Lemassu, M.-A. Laneelle, F. Bardou, G. Silve, P. Gounon, G. Marchal, and M. Daffé, "Identification of the surface-exposed lipids on the cell envelopes of *Mycobacterium tuberculosis* and other mycobacterial species.," *Journal of bacteriology*, vol. 178, no. 2, pp. 456–461, 1996.

[70] J. Chua, I. Vergne, S. Master, and V. Deretic, "A tale of two lipids: *Mycobacterium tuberculosis* phagosome maturation arrest," *Current opinion in microbiology*, vol. 7, no. 1, pp. 71–77, 2004.

[71] G. R. Strohmeier and M. J. Fenton, "Roles of lipoarabinomannan in the pathogenesis of tuberculosis," *Microbes and infection*, vol. 1, no. 9, pp. 709–717, 1999.

[72] V. Briken, S. A. Porcelli, G. S. Besra, and L. Kremer, "Mycobacterial lipoarabinomannan and related lipoglycans: from biogenesis to modulation of the immune response," *Molecular microbiology*, vol. 53, no. 2, pp. 391–403, 2004.

[73] Y. Yamazaki, L. Danelishvili, M. Wu, M. MacNab, and L. E. Bermudez, "*Mycobacterium avium* genes associated with the ability to form a biofilm," *Applied and environmental microbiology*, vol. 72, no. 1, pp. 819–825, 2006.

[74] S. Hunter, R. Murphy, K. Clay, M. Goren, and P. Brennan, "Trehalose-containing lipooligosaccharides. a new class of species-specific antigens from *Mycobacterium*," *Journal of Biological Chemistry*, vol. 258, no. 17, pp. 10481–10487, 1983.

[75] J. T. Belisle and P. J. Brennan, "Chemical basis of rough and smooth variation in mycobacteria.," *Journal of bacteriology*, vol. 171, no. 6, pp. 3465–3470, 1989.

[76] A. Lemassu, V. V. Lévy-Frébault, M.-A. Lanéelle, and M. Daffé, "Lack of correlation between colony morphology and lipooligosaccharide content in the *Mycobacterium tuberculosis* complex," *Microbiology*, vol. 138, no. 7, pp. 1535–1541, 1992.

[77] A. Burguière, P. G. Hitchen, L. G. Dover, L. Kremer, M. Ridell, D. C. Alexander, J. Liu, H. R. Morris, D. E. Minnikin, A. Dell, *et al.*, "LosA, a key glycosyltransferase involved in the biosynthesis of a novel family of glycosylated acyltrehalose lipooligosaccharides from *Mycobacterium marinum*," *Journal of Biological Chemistry*, vol. 280, no. 51, pp. 42124–42133, 2005.

[78] J. Yu, V. Tran, M. Li, X. Huang, C. Niu, D. Wang, J. Zhu, J. Wang, Q. Gao, and J. Liu, "Both phthiocerol dimycocerosates and phenolic glycolipids are required for virulence of *Mycobacterium marinum*," *Infection and immunity*, vol. 80, no. 4, pp. 1381–1389, 2012.

[79] M. B. Reed, P. Domenech, C. Manca, H. Su, *et al.*, "A glycolipid of hypervirulent tuberculosis strains that inhibits the innate immune response," *Nature*, vol. 431, no. 7004, p. 84, 2004.

[80] S. S. Branda, Å. Vik, L. Friedman, and R. Kolter, "Biofilms: the matrix revisited," *Trends in microbiology*, vol. 13, no. 1, pp. 20–26, 2005.

[81] A. K. Ojha, X. Trivelli, Y. Guerardel, L. Kremer, and G. F. Hatfull, "Enzymatic hydrolysis of trehalose dimycolate releases free mycolic acids during mycobacterial growth in biofilms," *Journal of Biological Chemistry*, vol. 285, no. 23, pp. 17380–17389, 2010.

[82] V. Rao, N. Fujiwara, S. A. Porcelli, and M. S. Glickman, "*Mycobacterium tuberculosis* controls host innate immune activation through cyclopropane modification of a glycolipid effector molecule," *Journal of Experimental Medicine*, vol. 201, no. 4, pp. 535–543, 2005.

[83] M. S. Glickman, J. S. Cox, and W. R. Jacobs, "A novel mycolic acid cyclopropane synthetase is required for cording, persistence, and virulence of *Mycobacterium tuberculosis*," *Molecular cell*, vol. 5, no. 4, pp. 717–727, 2000.

[84] C. B. Whitchurch, T. Tolker-Nielsen, P. C. Ragas, and J. S. Mattick, "Extracellular DNA required for bacterial biofilm formation," *Science*, vol. 295, no. 5559, pp. 1487–1487, 2002.

[85] T. Das, S. K. Kutty, N. Kumar, and M. Manefield, "Pyocyanin facilitates extracellular DNA binding to *Pseudomonas aeruginosa* influencing cell surface properties and aggregation," *PLoS One*, vol. 8, no. 3, p. e58299, 2013.

[86] E. S. Gloag, L. Turnbull, A. Huang, P. Vallotton, H. Wang, L. M. Nolan, L. Mililli, C. Hunt, J. Lu, S. R. Osvath, *et al.*, "Self-organization of bacterial biofilms is facilitated by extracellular DNA," *Proceedings of the National Academy of Sciences*, vol. 110, no. 28, pp. 11541–11546, 2013.

[87] S. Hannan, D. Ready, A. S. Jasni, M. Rogers, J. Pratten, and A. P. Roberts, "Transfer of antibiotic resistance by transformation with eDNA within oral biofilms," *FEMS Immunology & Medical Microbiology*, vol. 59, no. 3, pp. 345–349, 2010.

[88] A. Seper, V. H. Fengler, S. Roier, H. Wolinski, S. D. Kohlwein, A. L. Bishop, A. Camilli, J. Reidl, and S. Schild, "Extracellular nucleases and extracellular DNA play important roles in *Vibrio cholerae* biofilm formation," *Molecular microbiology*, vol. 82, no. 4, pp. 1015–1037, 2011.

[89] M. Allesen-Holm, K. B. Barken, L. Yang, M. Klausen, J. S. Webb, S. Kjelleberg, S. Molin, M. Givskov, and T. Tolker-Nielsen, "A characterization of DNA release in *Pseudomonas aeruginosa* cultures and biofilms," *Molecular microbiology*, vol. 59, no. 4, pp. 1114–1128, 2006.

[90] M. Asally, M. Kittisopikul, P. Rué, Y. Du, Z. Hu, T. Çağatay, A. B. Robinson, H. Lu, J. Garcia-Ojalvo, and G. M. Süel, "Localized cell death focuses mechanical forces during 3D patterning in a biofilm," *Proceedings of the National Academy of Sciences*, vol. 109, no. 46, pp. 18891–18896, 2012.

[91] J. M. Chen, G. J. German, D. C. Alexander, H. Ren, T. Tan, and J. Liu, "Roles of Lsr2 in colony morphology and biofilm formation of *Mycobacterium smegmatis*," *Journal of bacteriology*, vol. 188, no. 2, pp. 633–641, 2006.

[92] C. M. Sassetti, D. H. Boyd, and E. J. Rubin, "Comprehensive identification of conditionally essential genes in mycobacteria," *Proceedings of the National Academy of Sciences*, vol. 98, no. 22, pp. 12712–12717, 2001.

[93] S. Tabor, "Expression using the T7 RNA polymerase/promoter system," *Current protocols in molecular biology*, pp. 16–2, 1990.

[94] J. P. Murry, C. M. Sassetti, J. M. Lane, Z. Xie, and E. J. Rubin, "Transposon site hybridization in *Mycobacterium tuberculosis*," *Microbial Gene Essentiality: Protocols and Bioinformatics*, pp. 45–59, 2008.

[95] M. Vuoksio, "Zebrafish model for mycobacterial infection," 2011.

[96] "MarinoList." `http://mycobrowser.epfl.ch/marinolist.html`, 2010. Accessed October 13th 2017.

[97] J. Dolezel, J. Bartos, H. Voglmayr, and J. Greilhuber, "Nuclear DNA content and genome size of trout and human.," *Cytometry. Part A: the journal of the International Society for Analytical Cytology*, vol. 51, no. 2, pp. 127–8, 2003.

[98] E. Peeters, H. J. Nelis, and T. Coenye, "Comparison of multiple methods for quantification of microbial biofilms grown in microtiter plates," *Journal of microbiological methods*, vol. 72, no. 2, pp. 157–165, 2008.